Linear Kondo conductance in a quantum dot

2004 J. Phys.: Condens. Matter 16 S1453

(http://iopscience.iop.org/0953-8984/16/17/003)

INSTITUTE OF PHYSICS PUBLISHING JOURNAL OF PHYSICS: CONDENSED MATTER

J. Phys.: Condens. Matter **16** (2004) S1453–S1483 PII: S0953-8984(04)64559-0

Linear Kondo conductance in a quantum dot

Domenico Giuliano[1], **Adele Naddeo**[2,3] **and Arturo Tagliacozzo**[2,3]

[1] Dipartimento di Fisica, Università della Calabria, Arcavacata di Rende, Cosenza, Italy
[2] Coherentia—INFM (Istituto Nazionale di Fisica della Materia), Unità di Napoli, Napoli, Italy
[3] Dipartimento di Scienze Fisiche, Università di Napoli 'Federico II', Monte S Angelo, via Cintia, I-80126 Napoli, Italy

Received 6 June 2003
Published 16 April 2004
Online at stacks.iop.org/JPhysCM/16/S1453
DOI: 10.1088/0953-8984/16/17/003

Abstract

In a tunnelling experiment across a quantum dot it is possible to change the coupling between the dot and the contacts at will, by properly tuning the transparency of the barriers and the temperature. Gate voltages allow for changes of the relative position of the dot addition energies and the Fermi level of the leads. Here we discuss the two limiting cases: weak and strong coupling in the tunnelling Hamiltonian. In the latter case Kondo resonant conductance can emerge at low temperature in a Coulomb blockade valley. We give a pedagogical approach to the single-channel Kondo physics at equilibrium and review the Nozières scattering picture of the correlated fixed point. We emphasize the effect of an applied magnetic field and show how an orbital Kondo effect can take place in vertical quantum dots tuned both to an even and to an odd number of electrons at a level crossing. We extend the approach to the two-channel overscreened Kondo case and discuss recent proposals for detecting the non-Fermi liquid fixed point which could be reached at strong coupling.

(Some figures in this article are in colour only in the electronic version)

1. Introduction

Recently systems have been fabricated which can sustain quantum coherence because of the smallness of their size, provided that the temperature is low enough. These mesoscopic systems are nanostructured devices in which quantum coherence sets in at very low temperatures and modifies the properties of the device as a whole. This happens notwithstanding the fact that the system is connected to an external biasing circuit. They have global, geometry dependent properties and striking quantization phenomena arise which are largely independent of the specific sample involved: charge quantization (in units of the electron charge e), periodicity in the magnetic flux quantum $\phi_0 = hc/e$, conductance quantization (in units of $G_K = 2e^2/\pi\hbar = (6.5\,\mathrm{k}\Omega)^{-1}$).

Among these macroscopic quantum phenomena there is the unitary limit of the Kondo conductance in tunnelling across a quantum dot (QD) at Coulomb blockade (CB) [1, 2] that was first measured in 1998 [3]. The Kondo phenomenon has been well known since the 1960s and explains an anomaly in the temperature dependence of the resistivity of dilute magnetic alloys [4, 5].

This review is devoted to some features of equilibrium Kondo conductance across a quantum dot in the CB regime interacting with two contacts. It is remarkable here that the dot acts as a single impurity probed by the metal contacts, so the properties of the Kondo state are not mediated over many impurities per cubic centimetre as happens in dilute magnetic alloys. A strongly coupled state sets in between the dot and the contacts and phase coherence is established among the conduction electrons and the whole structure.

The temperature scale for the interactions between a magnetic impurity and the delocalized conduction electrons of the host metal is the so-called Kondo temperature T_K. It is defined as the temperature at which the perturbative analysis breaks down. Therefore, different approaches are required to investigate the thermodynamics and the transport properties of a quantum dot in the Kondo regime over the whole range of temperatures from the perturbative region down to the unitarity limit.

Recently, the Kondo model and the Anderson impurity model in its Kondo limit have been investigated in depth by means of numerical renormalization group (NRG) calculations [6], the Bethe ansatz method [7] and conformal field theory (CFT) techniques [8]. Further developments in the NRG methods have been applied successfully in the crossover region $T \approx T_K$ [9]. The zero-field spectral and transport properties of the Anderson model in the Kondo regime [10] as well as the field and temperature dependence of the Kondo resonance and the equilibrium magnetoconductance of the dot [11] have been investigated. The tunnelling conductance as a function of the gate voltage has also been calculated using the NRG, over a wide temperature range for a single quantum dot with Coulomb interactions, assuming that two orbitals were active for the tunnelling process [12].

We leave out the case where the electron distribution is not in local equilibrium about the Kondo impurity and the linear response theory is no longer sufficient. A number of techniques have been applied to describe non-equilibrium properties such as the non-linear conductance, the non-equilibrium stationary state and the full time development of an initially out-of-equilibrium system: variational calculations [13], perturbation theory [14], equations of motion [15], perturbative functional integral methods [16], the non-crossing approximation (NCA) [17, 18], the perturbative renormalization group (RG) method in real time [19]. In particular, the last technique is well suited for describing quantum fluctuations which are induced by strong coupling between a small quantum system and an environment. It succeeds in reproducing the anomalous line shapes of the conductance observed in several recent experiments [3], due to the renormalization of the resistance and the local energy excitations [20].

We also leave out situations in which the levels localized at the dot are close in energy to the Fermi energy of the contacts (mixed valence models).

The plan of the paper is the following. We start from the tunnelling Hamiltonian formalism when the coupling between the dot and the contacts is weak (section 2). A scattering approach in one dimension is particularly suitable when studying the linear conductance in the device. The prototype model for accounting for strong electron–electron repulsion on the dot is the Anderson Hamiltonian with on-site repulsion (section 3). In the limit of strong correlation between the dot and the leads the latter model maps onto the so-called 'Kondo Hamiltonian model' (section 4). A *poor man's scaling* approach up to second order leads us to the definition of the Kondo temperature T_K. Next, we introduce the physics of the single-channel (section 6)

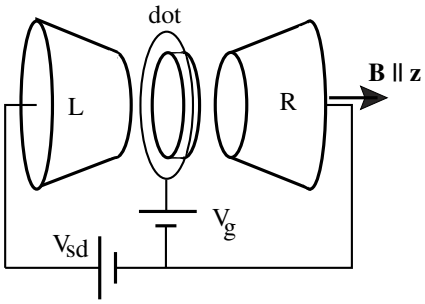

Figure 1. A schematic drawing for a dot and the contacts in a vertical set-up; possibly a magnetic field is applied along the axis.

and the two-channel Kondo problem (section 7), both in the perturbative region and in the unitarity limit. In this context we briefly sketch the Anderson *et al* [21] Coulomb gas approach to the isotropic and anisotropic one-channel Kondo system which gives straightforward, though qualitative, insight into the strongly correlated state.

In the conventional setting the dynamical variable which is coupled to the electrons propagating from the leads is the total dot spin. There are cases in which the spin is locked to orbital degrees of freedom or even absent ('orbital Kondo') [22]; such cases are better found in a vertical geometry in the presence of a magnetic field orthogonal to the dot [23]. A rather strong vertical magnetic field can induce level crossings in the dot due to orbital effects and produce accidental degeneracies which can give rise to exotic Kondo couplings (see sections 6.2 and 6.3). Some attention is drawn to the cylindrical geometry and to symmetry selection rules in the cotunnelling process, and also in connection with proposals for achieving the two-channel Kondo non-Fermi liquid fixed point in a vertical dot device [24–26] (section 7.3).

2. The tunnelling Hamiltonian at weak coupling

Quantum dots (QD) are fabricated in semiconductor heterostructures, by applying metallic gates to confine a few electrons [27]. Because the confining area is quite small (the radius is $\sim$100–1000 Å), the charging energy is much larger than the energy associated with thermal fluctuations, provided that the temperature is below 1 K. Therefore the dot is only weakly linked to metal contacts and one can bias the system in such a way that the electron number N in the dot can be changed at will. Because of the confining potential, dots display a level structure organized in shells, exactly as atoms do. Analysing this level structure is of primary interest because these few interacting electrons ($N \leqslant 20$) confined in a disc-like box (see figure 1), at special values of the parameters, are ruled by strong many-body Coulomb correlations. Hund's rules can be seen at work: the total spin S of the electrons confined in the dot is maximized as long as no magnetic field is applied. On the other hand, a magnetic field in the direction orthogonal to the disc produces strong orbital effects which favour larger values of the total angular momentum M as well as total spin S.

Quantum dots are remarkable because of Coulomb oscillations. At very low temperature, the linear conductance (at vanishing bias $V_{\rm sd}$) is zero, except for peaks at discrete values of the gate voltage $V_{\rm g}$, when it is energetically favourable to add one extra electron to the dot. Therefore $V_{\rm g}$ controls the number of particles on the dot in the CB regime.

We tune the chemical potential μ of the left (L) and right (R) bulk contacts within the CB valley of the conductance at N particles, that is $\mu_N < \mu < \mu_{N+1,\alpha} \equiv {}^{N+1}E_\alpha - {}^{N}E_0$; here

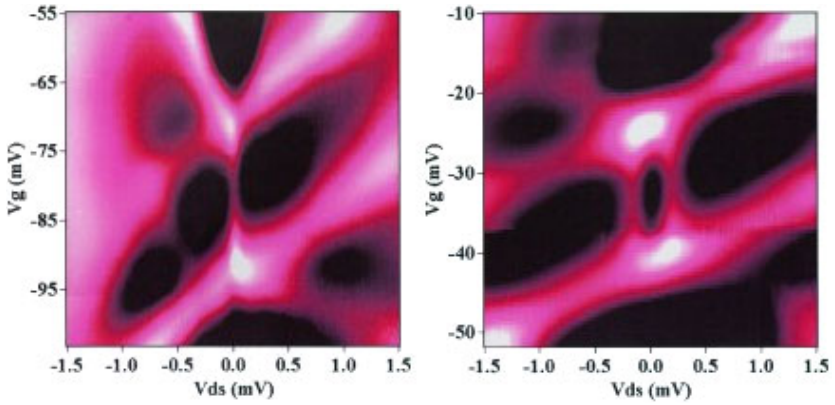

Figure 2. Differential conductance on a greyscale as a function of both V_g and V_{ds}; the Kondo effect shows up near $V_{ds} = 0$ [29].

the energies ${}^{N\pm1}E_\alpha$ are the total energies for the dot with $N \pm 1$ particles characterized by the quantum numbers α and ${}^{N}E_0$ is the ground state energy (GS) at N particles. If N is odd, then the GS is at least doubly degenerate because the odd particle state can have spin $\sigma = \uparrow, \downarrow$. In this case the dot can be treated as a single Anderson impurity.

The peculiarity of these artificial atoms is in that the level structure can be investigated by measuring the tunnelling current. Peaks in the linear conductance versus gate voltage V_g separate regions at Coulomb blockade (CB) in which N is fixed and differs by just one electron. The peaks at zero source–drain voltage occur whenever V_g compensates the required chemical potential for electron addition or subtraction. Hence, measuring a tunnel current across the device versus V_g provides the spectroscopy of the dot levels. Adding a magnetic field, the spin state of the dot can be changed, which in turn changes the selection rules for electron tunnelling [28].

The height and the width of the conductance peaks at resonance depend on temperature T. Let the dimensionless conductance be g (in units of $2\frac{e^2}{h}$ (the factor of 2 is for the spin)). In the simplest case the maximum of the conductance at the resonant peak is $g_{\max} \propto \Gamma/(k_B T)$ and the half-width of the peak $\Gamma = \pi\nu(0)|V|^2$ is $\propto T$; here V is the tunnelling strength (see below) and $\nu(0)$ is the density of states at the Fermi energy. In the CB region, tunnelling via virtual states of the dot with $N \pm 1$ is only fourth-order perturbation in V (these are named cotunnelling processes), $g \propto e^2\pi(\frac{2\nu(0)|V|^2}{\epsilon_d})^2/\hbar$, and vanishes exponentially with reducing temperature.

Nevertheless, unexpectedly, transport measurement in a dot gives rise to some new physics which can be related to the Kondo effect of spin impurities in non-magnetic metal alloys (see figure 2) [3].

In the following we introduce the model for a quantum dot interacting with the contacts and define an equivalent one-dimensional Hamiltonian.

2.1. Current within the tunnelling Hamiltonian

In this subsection we discuss the mutual influence between the contacts and the dot, starting from the weak link limit. Conduction electrons in the leads constitute a Fermi sea (FS) of non-interacting fermions with plane wave single-particle wavefunctions on side L and on side R. The dot is described by a Hamiltonian H_D and coupling between the dot and the leads is

accounted for through a tunnelling term, so the Hamiltonian describing the whole system is

$$H = H_{\mathrm{D}} + \sum_{k\sigma} \epsilon^{\mathrm{R}}_{k\sigma} a^{\dagger}_{k\sigma} a_{k\sigma} + \sum_{k\sigma} \epsilon^{\mathrm{L}}_{k\sigma} b^{\dagger}_{k\sigma} b_{k\sigma} + \sum_{k\alpha\sigma} [V_{k\alpha} c^{\dagger}_{k\alpha\sigma} d_{\sigma} + V^{*}_{k\alpha} d^{\dagger}_{\sigma} c_{k\alpha\sigma}]. \quad (1)$$

The right and left Fermi seas (FS) of the two contacts R, L are acted on by operators $c_{k\mathrm{R}\sigma} \equiv a_{k\sigma}$ and $c_{k\mathrm{L}\sigma} \equiv b_{k\sigma}$ (here the index α stands for R, L). The canonical transformation of the dot problem by Glazman and Raikh [1] is just the construction of two species of fermions whose wavefunction is even or odd with respect to the dot centre, in the case where the two barriers are unequal: $V_{\alpha} = V_{\mathrm{R}}, V_{\mathrm{L}}$. This changes the picture from operators $a_{k\sigma}$ and $b_{k\sigma}$ to operators $\alpha_{k\sigma}$ and $\beta_{k\sigma}$ given by

$$\begin{aligned} &\alpha_{k\sigma} = u a_{k\sigma} + v b_{k\sigma}, \qquad \beta_{k\sigma} = u b_{k\sigma} - v a_{k\sigma}, \\ &u = \frac{V_{\mathrm{R}}}{V}, \qquad v = \frac{V_{\mathrm{L}}}{V}, \qquad V = \sqrt{|V_{\mathrm{R}}|^2 + |V_{\mathrm{L}}|^2}, \qquad \Gamma_{R,L} = \pi |V_{R,L}|^2 \nu(0), \end{aligned} \quad (2)$$

where $\nu(0)$ is the density of states at the Fermi energy.

A general formula for the conductance of interacting systems [30, 15, 31] has been written, resorting to the non-equilibrium Keldysh formalism [32]; in such a framework the current through the interacting region is written in terms of the distribution functions in the leads and local properties of the intermediate region, such as the occupation and the density of states at the dot site:

$$J = \frac{\mathrm{i}e}{2h} \int \mathrm{d}\omega \, (\mathrm{Tr}\{2[f_{\mathrm{L}}(\omega)\Gamma_{\mathrm{L}} - f_{\mathrm{R}}(\omega)\Gamma_{\mathrm{R}}](\mathbf{G}^{\mathrm{r}} - \mathbf{G}^{\mathrm{a}})\} + \mathrm{Tr}\{2(\Gamma_{\mathrm{L}} - \Gamma_{\mathrm{R}})\mathbf{G}^{<}\}), \quad (3)$$

where $\mathbf{G}^{\mathrm{r}}$, $\mathbf{G}^{\mathrm{a}}$, $\mathbf{G}^{<}$ are the usual retarded, advanced, Keldysh Green functions for the dot in interaction with the leads and the f are the Fermi functions. The Green function $\mathbf{G}^{\mathrm{r}}$ will be denoted as G_{dd} in the following. Both $\mathbf{G}^{\mathrm{r}}$ and $\Gamma_{\mathrm{R,L}}$ are matrices in the case where many channels are present.

Formula (3) can be cast in a simpler form in the case where the couplings to the leads differ only by a constant factor [15]:

$$J = -2\frac{e}{h} \int \mathrm{d}\omega \, [f_{\mathrm{L}}(\omega) - f_{\mathrm{R}}(\omega)] \, \mathrm{Im}\, \mathrm{Tr}\{\tilde{\Gamma} \mathbf{G}^{\mathrm{r}}(\omega)\}, \quad (4)$$

where $\tilde{\Gamma} = \Gamma_{\mathrm{R}}\Gamma_{\mathrm{L}}/\Gamma$. Here $\Gamma = \Gamma_{\mathrm{R}} + \Gamma_{\mathrm{L}}$.

Now we derive explicitly G_{dd} within the lowest order perturbation in the tunnelling.

We start from the Hamiltonian in equation (1), where H_{D} is given by a single-impurity energy level ϵ_d. All quantities will be scalar quantities for simplicity. We define the electron retarded Green function for the unperturbed leads: $G_0^{-1} = \sum_k (\omega - \epsilon_k + \mathrm{i}0^{+})$. Projecting the equations for the total Green function:

$$\begin{aligned} &(\mathrm{i}\omega_n - H) G(\mathrm{i}\omega_n) = \mathbf{1}, \\ &G^{\dagger}(\mathrm{i}\omega_n)(-\mathrm{i}\omega_n - H) = \mathbf{1}, \end{aligned} \quad (5)$$

onto states in which one single extra particle is occupying the delocalized state $|k\rangle$ or the impurity state $|d\rangle$, we have

$$\begin{aligned} &(\mathrm{i}\omega_n - \epsilon_k) G_{k,k'\sigma}(\mathrm{i}\omega_n) = \delta_{kk'} + V_k G_{d,k'\sigma}(\mathrm{i}\omega_n), \\ &G_{d,k'\sigma}(\mathrm{i}\omega_n)(-\mathrm{i}\omega_n - \epsilon_{k'}) = G_{d,d\sigma}(\mathrm{i}\omega_n) V^{*}_{k'}, \end{aligned} \quad (6)$$

where $G_{d,k\sigma}(\mathrm{i}\omega_n) = \langle d|G|k\rangle$, $G_{k,k\sigma}(\mathrm{i}\omega_n) = \langle k|G|k\rangle$, $G_{d,d\sigma}(\mathrm{i}\omega_n) = \langle d|G|d\rangle$ and $V_k = \langle k|V|d\rangle$.

This gives for each scattering channel (here in order to simplify the notation we suppress the channel label α)

$$\begin{aligned} G_{k,k'\sigma}(\mathrm{i}\omega_n) &= \frac{\delta_{kk'}}{\mathrm{i}\omega_n - \epsilon_k} + \frac{V_k}{\mathrm{i}\omega_n - \epsilon_k} G_{d,d\sigma}(\mathrm{i}\omega_n) \frac{V^{*}_{k'}}{\mathrm{i}\omega_n - \epsilon_{k'}} \\ &\equiv G^{0}_{k\sigma}\delta_{kk'} + G^{0}_{k\sigma} V_k G_{d,d\sigma} V^{*}_{k'} G^{0}_{k'\sigma'}. \end{aligned} \quad (7)$$

The density of states of the scattering electrons is defined as

$$\nu(\omega) = -\frac{1}{\pi}\,\mathrm{Im}\sum_k \mathbf{G}^{\mathrm{r}}_{k,k\sigma}(\omega). \tag{8}$$

Using similar equations for the dot, we write

$$G_{d,d\sigma}(\mathrm{i}\omega_n) = \frac{1}{\mathrm{i}\omega_n - \epsilon_d - \sum_k |V_k|^2/(\mathrm{i}\omega_n - \epsilon_k)}. \tag{9}$$

Now, let us consider the L and R contacts as two equal Fermi gases of non-interacting particles and equal chemical potential $\mu = 0$ (within the linear conductance regime a source–drain voltage V_{sd} is not applied). In such a case it is enough to discuss a single effective contact and the corresponding wavefunctions are plane waves of wavevector k in the x direction with a label α which includes all other quantum numbers. Their energy dispersion $\epsilon_{k\alpha}$ can be linearized about μ with $\epsilon_q \approx \hbar v_{\mathrm{F}} q$, where q is the momentum measured with respect to the Fermi momentum and v_{F} is the Fermi velocity. Using a constant density of states $\nu(0)$ (at the Fermi energy per spin $L_0/2\pi\hbar v_{\mathrm{F}}$ where L_0 is the size of the system) and a bandwidth of size $2D$ and neglecting the k dependence of V_k, the sum in equation (9) is readily carried out:

$$\sum_k \frac{|V_k|^2}{\mathrm{i}\omega_n - \epsilon_k} = |V|^2\nu(0)\int_{-D}^{D} \mathrm{d}\epsilon\, \frac{1}{\mathrm{i}\omega_n - \epsilon} = \frac{\Gamma}{\pi}\ln\frac{\mathrm{i}\omega_n + D}{\mathrm{i}\omega_n - D} \equiv \Sigma_d(\mathrm{i}\omega_n). \tag{10}$$

The retarded Green function for the dot is obtained from $G_{d,d\sigma}(\mathrm{i}\omega_n)$ in the limit of real frequencies: $\mathrm{i}\omega_n \to \omega + \mathrm{i}0^+$ according to

$$\mathbf{G}^{-1}_{d,d\sigma}(\mathrm{i}\omega_n) = \{\mathrm{i}\omega_n - \epsilon_d - \Sigma_d(\mathrm{i}\omega_n)\} \to \omega - \epsilon_d - \frac{\Gamma}{\pi}\ln\left|\frac{v_{\mathrm{F}}D + \omega}{v_{\mathrm{F}}D - \omega}\right| + \mathrm{i}\Gamma = \omega - \tilde{\epsilon}_d + \mathrm{i}\Gamma, \tag{11}$$

where $\tilde{\epsilon}_d$ is the renormalized dot energy. The coupling of the dot to the contacts shifts the location of the pole corresponding to the energy of the localized level and gives a finite width Γ to the resonance.

2.2. 1D scattering formalism

At zero temperature, scattering is only elastic. In the following we develop a 1D scattering approach which is mostly useful in vertical structures [33]; next we show that the tunnelling conduction can also be cast into the scattering form.

If the evolution operator $U(t, t')$ is known, the transmission amplitude can be written in a scattering approach as $\theta^{\mathrm{R}\to\mathrm{L}} = \langle b^\dagger U(+\infty, -\infty)a\rangle = v^* u\langle\alpha^\dagger(\infty)\alpha(-\infty)\rangle - u^* v\langle\beta^\dagger(\infty)\beta(-\infty)\rangle \equiv v^* u S^0 + u^* v S^1$, where we have defined the two expectation values as the scattering matrix elements for the two uncoupled even and odd channels. Hence, the conductance takes the form of the Landauer formula:

$$g = T^{\mathrm{R}\to\mathrm{L}} \equiv |\theta^{\mathrm{R}\to\mathrm{L}}|^2 = 4|v^* u|^2\left|\frac{1}{2}\sum_l S^l\right|^2 = \frac{4\Gamma_{\mathrm{R}}\Gamma_{\mathrm{L}}}{(\Gamma_{\mathrm{R}} + \Gamma_{\mathrm{L}})^2}\left|\frac{1}{2}\sum_l S^l\right|^2. \tag{12}$$

The potential after the transformation of equation (2) has become even; hence unitarity is satisfied by each channel individually: $|S^l|^2 = 1, l = 0, 1$. The unitary limit of the conductance is $g_{\mathrm{u}} = \frac{4\Gamma_{\mathrm{R}}\Gamma_{\mathrm{L}}}{(\Gamma_{\mathrm{R}}+\Gamma_{\mathrm{L}})^2}$. In particular, if the potential is $\delta(x)$, odd parity is totally transmitted and such that $S^1 = -1$.

Equation (12) is valid for a general system with an interacting intermediate region. One can match this approach to a 1D scattering approach for non-interacting electrons as is done here, below.

Let us place the impurity (QD) at $x = 0$ and consider the scattering amplitude $f_{\mathrm{L,R}}$ of a one-electron wavefunction $\psi(x)$:

$$\begin{aligned} &\psi_{>}(x) \propto \mathrm{e}^{\mathrm{i}kx} + f_{\mathrm{R}}\mathrm{e}^{\mathrm{i}kx}, \qquad x \gg 0, \\ &\psi_{<}(x) \propto \mathrm{e}^{\mathrm{i}kx} + f_{\mathrm{L}}\mathrm{e}^{-\mathrm{i}kx}, \qquad x \ll 0. \end{aligned} \tag{13}$$

Here the transmission coefficient is $T = |1 + f_{\mathrm{R}}|^2$ while the reflection coefficient is $R = |f_{\mathrm{L}}|^2$ and they satisfy the conservation of flux: $T + R = 1$.

If the dot structure is even with respect to the origin along the vertical axis, the even parity $l = 0$ and the odd parity $l = 1$ channels are independent. It is then useful to define even and odd parities f^l: $f^0 = \frac{1}{2}(f_{\mathrm{L}} + f_{\mathrm{R}})$, $f^1 = \frac{1}{2}(f_{\mathrm{R}} - f_{\mathrm{L}})$ and the elastic t matrix $t^l = \mathrm{i}k_0 f^l/\pi$. Here the energy of the incoming particle is $\hbar v_{\mathrm{F}} k_0$ (in units of $\hbar v_{\mathrm{F}} = 1$; it follows that $[t] =$ energy) and $k_0 = 2\pi/L_0$ (where L_0 is the linear size of the system). The t matrix is related to the S matrix according to

$$\begin{aligned} &S^l = \mathrm{e}^{2\mathrm{i}\delta^l}; \qquad S^l - 1 = -\frac{2\pi\mathrm{i}}{k_0}t^l, \\ &t^l = -\frac{k_0}{\pi}\sin\delta^l \mathrm{e}^{\mathrm{i}\delta^l}, \end{aligned} \tag{14}$$

where the δ^l are the phase shifts for the two parities. In this context, the unitarity of the S matrix, $\frac{1}{2}\sum_l |S^l|^2 = 1$, is the same as the flux conservation $R + T = 1$.

The conductance is given by the Landauer formula:

$$\text{conductance} = g = T = |1 + f_{\mathrm{R}}|^2 = \left|1 + \mathrm{i}\sum_l \sin\delta^l \mathrm{e}^{\mathrm{i}\delta^l}\right|^2. \tag{15}$$

In the case of resonant tunnelling we have $T \sim 1$ and $R = |f_{\mathrm{L}}|^2 \sim 0$, so equation (15) becomes $g \to 1$—that is, the unitary limit.

The condition $R = |\pi(t^0 - t^1)/(\mathrm{i}k_0)|^2 = \sin^2(\delta^0 - \delta^1) \sim 0$ yields $\delta^0 \sim \delta^1 \equiv \delta \bmod \pi$, while in equation (15) we have $T \sim 1$ for $\delta^0 = \delta^1 \equiv \delta \to \pi/2$.

If the potential is even ($\Gamma_{\mathrm{R}} = \Gamma_{\mathrm{L}}$), unitarity is satisfied by each channel individually: $|S^l|^2 = 1$, $l = 0, 1$; in particular, if the potential is $\delta(x)$, odd parity is totally transmitted and such that $S^1 = -1$, and the conductance becomes

$$g = \left|\frac{1}{2}(S^0 - 1)\right|^2 = \left|\frac{\pi}{k_0}t^0\right|^2 = \sin^2\delta^0. \tag{16}$$

Again, if $\delta^0 = \pi/2$, the conductance reaches the unitarity limit.

In the following we describe the basic approximations and the weak coupling limit of very opaque barriers between the dot and contacts.

In this case tunnelling of lead electrons across the dot is a perturbative process as derived in section 2.1. Within such a perturbative regime neither the dot nor the contacts are much affected by the interaction with the other. The relevant effect on the QD is the shifting of its levels and a level broadening, which is a second-order effect in the tunnelling strength V. This shows itself as a small imaginary part added to the energy levels, i.e. a finite lifetime.

It is easy to show that the linear conductance given above can be rephrased in terms of the imaginary part of the Green function as in equation (4) at the perturbative level. To this end, let us first state some formalities regarding the self-energy $\mathbf{\Sigma}$ and the $\mathbf{t}$ matrix:

$$(E - H_0 - \Sigma)\mathbf{G} = \mathbf{1}; \qquad \mathbf{G}_0(E - H_0) = \mathbf{1} \to \mathbf{G}_0\mathbf{G}^{-1} + \mathbf{G}_0\mathbf{\Sigma} = \mathbf{1} \to \mathbf{G} = \mathbf{G}_0 + \mathbf{G}_0\mathbf{\Sigma}\mathbf{G}.$$

In the Born approximation Σ and $\mathbf{t}$ coincide because by definition $\mathbf{G} = \mathbf{G}_0 + \mathbf{G}_0\mathbf{t}\mathbf{G}_0$. We assume that in tunnelling the odd parity channel is fully transmitted ($S^1 = -1$) and the even parity one gives (see equation (7))

$$t^0 \sim V G_{d,d} V, \qquad G_{d,d} = \frac{1}{\epsilon - \tilde{\epsilon}_0 + \mathrm{i}\Gamma}$$
$$\to t^0 \sim \frac{|V|^2}{\epsilon - \tilde{\epsilon}_0 + \mathrm{i}\Gamma}, \qquad \frac{\mathrm{Im}\, t^0}{\mathrm{Re}\, t^0} = \tan\delta^0 = \frac{-\Gamma}{\epsilon - \tilde{\epsilon}_0}, \tag{17}$$
$$\sin^2\delta^0 = \frac{\tan^2\delta^0}{1+\tan^2\delta^0} = \frac{\Gamma^2}{(\epsilon-\tilde{\epsilon}_0)^2+\Gamma^2}.$$

Here V is the tunnelling matrix element defined in equation (2), $\tilde{\epsilon}_0$ is the renormalized quantity defined in equation (11) and $\Gamma = \Gamma_\mathrm{R} + \Gamma_\mathrm{L}$ is the inverse lifetime of the resonance. This implies that equations (12), (16) become

$$g = g_\mathrm{u} \sin^2\delta^0 = \frac{4\Gamma_\mathrm{R}\Gamma_\mathrm{L}}{(\epsilon-\tilde{\epsilon}_0)^2+\Gamma^2}, \tag{18}$$

where $g_\mathrm{u} = \frac{4\Gamma_\mathrm{R}\Gamma_\mathrm{L}}{(\Gamma_\mathrm{R}+\Gamma_\mathrm{L})^2}$. On the other hand, because $\mathrm{Im}\, G = -\Gamma/[(\epsilon-\tilde{\epsilon}_0)^2+\Gamma^2]$, equation (4) becomes

$$g = \int \mathrm{d}\omega \left(-\frac{\partial f(\omega)}{\partial\omega}\right)\tilde{\Gamma}\frac{\Gamma}{(\epsilon-\tilde{\epsilon}_0)^2+\Gamma^2}, \tag{19}$$

where $\tilde{\Gamma} = \Gamma_\mathrm{R}\Gamma_\mathrm{L}/\Gamma$. At zero temperature the results of equations (18) and (19) coincide.

At finite temperature, if the odd channel is fully transmitted, equation (12) can be generalized as

$$g = g_\mathrm{u} \int \mathrm{d}\omega \left(-\frac{\partial f(\omega)}{\partial\omega}\right)[-\pi\nu(0)\,\mathrm{Im}(t^0)] \tag{20}$$

where t^0 is the **t** matrix defined above and related to the exact retarded Green function through the relation $\mathbf{G} = \mathbf{G}_0 + \mathbf{G}_0\mathbf{t}\mathbf{G}_0$. We have used the optical theorem:

$$\frac{\pi^2}{k_0^2}\,\mathrm{Tr}\{t^0 t^{0\dagger}\} = \mathrm{Re}\left\{\frac{\mathrm{i}\pi}{k_0}t^0\right\} \tag{21}$$

which follows from the unitarity condition $|S^0|^2 = 1$.

3. The role of the on-site repulsion U in tunnelling

Up to now, H_D referred just to a single impurity level ϵ_d. Indeed, the charging energy U is the main feature of a QD and we have to deal with it. Something which is closer to a QD is an impurity level with on-site repulsion U. Inclusion of U in the Hamiltonian (1) leads to the single-level Anderson model:

$$H_\mathrm{AND} = H_\mathrm{lead} + \epsilon_d \sum_\sigma n_\sigma + U \sum_{\sigma\sigma'} n_\sigma n_{\sigma'} + \sum_{k\alpha\sigma} V_\alpha [c^\dagger_{k\alpha\sigma} d_\sigma + d^\dagger_\sigma c_{k\alpha\sigma}]. \tag{22}$$

If $\epsilon_d = -U/2$ with respect to the chemical potential of the conduction electrons μ (taken as the zero of the single-particle energies), the Anderson model which arises is symmetric. In fact, the energies of the empty impurity state, ${}^0E$, and of the doubly occupied impurity state, ${}^2E = 2\epsilon_d + U$, are both zero, while the singly occupied impurity level has energy ${}^1E = -U/2$.

In order to understand how the Coulomb repulsion on the dot site affects the Green function of the dot we use a path integral formalism. We show that, in the limit in which the charge degree of freedom on the dot is frozen ($U \to \infty$), the dot Green function describes the dynamics of the only degree of freedom left, that is the dot magnetization $\langle n_\uparrow - 1/2\rangle \equiv \langle 1/2 - n_\downarrow\rangle$ which is forced by a stochastic field $X(\tau)$ in imaginary time, produced by the scattering of the lead electrons, with a Gaussian probability distribution. The excitation energy associated with it is

shifted from ϵ_d to the Fermi level: this is the origin of the resonance at the Fermi level in the Kondo problem.

As a first step, we will rephrase the previous result of an impurity with $U = 0$ in this new approach. After linearizing the bands, the leads action can be written in terms of the field operators $\psi_{u\alpha}$ (where $\alpha = \mathrm{L}, \mathrm{R}$ and u includes all other quantum numbers) as

$$S_{\mathrm{lead}} = -\mathrm{i}v_{\mathrm{F}} \int_0^\beta \mathrm{d}\tau \int \mathrm{d}x \sum_u \sum_{\alpha=\mathrm{L},\mathrm{R}} \psi^\dagger_{u\alpha}(x,\tau) \frac{\mathrm{d}}{\mathrm{d}x} \psi_{u\alpha}(x,\tau). \tag{23}$$

With respect to the tunnelling action, if the L and R barriers are equal and the dot is zero dimensional, the interaction term only includes the symmetric combinations $\Phi_u(\tau) = \frac{1}{\sqrt{2}}(\psi_{uL}(x=0,\tau) + \psi_{uR}(x=0,\tau))$ at the origin:

$$S_{\mathrm{T}} = \int_0^\beta \mathrm{d}\tau \, \sqrt{2} \sum_u [V \Phi^\dagger_u(\tau) d_u(\tau) + V^* d^\dagger_u(\tau) \Phi_u(\tau)]. \tag{24}$$

The total action is

$$\mathcal{A} = \int_0^\beta \mathrm{d}\tau \left\{ \sum_u d^\dagger_u(\tau) \left[\frac{\partial}{\partial \tau} + (\epsilon_d - \mu) \right] d_u(\tau) \right\} + S_{\mathrm{lead}} + S_{\mathrm{T}}. \tag{25}$$

One can first integrate out the degrees of freedom of the $\psi_{u\alpha}(\tau, x)$ fields for $x \neq 0$ which are free-like, and next the field Φ_u at $x = 0$ which is the only one interacting with the dot variable $d_u(\tau)$. Because the fields in the leads are non-interacting, the result of the Gaussian integration yields an effective action for the dot:

$$-S^{\mathrm{Eff}}_{\mathrm{D}} \propto \ln \left\{ \int \prod_{\alpha=\mathrm{L},\mathrm{R}} \prod_u \mathcal{D}\psi_{u\alpha} \mathcal{D}\psi^\dagger_{u\alpha} \mathrm{e}^{-\mathcal{A}} \right\} = -\beta \sum_{\mathrm{i}\omega_n} d^\dagger_u(\mathrm{i}\omega_n)(\mathrm{i}\omega_n - \epsilon_d - \Sigma(\mathrm{i}\omega_n)) d_u(\mathrm{i}\omega_n), \tag{26}$$

where the self-energy correction to the Green function of the dot $\Sigma(\mathrm{i}\omega_n) = \frac{\Gamma}{\pi} \ln(\frac{\mathrm{i}\omega_n + D}{\mathrm{i}\omega_n - D})$ was obtained in equation (10).

3.1. Coulomb repulsion on the dot: freezing of the charge degree of freedom

We now discuss the role of the on-site Coulomb interaction. In the large U limit we have

$$\begin{aligned} \exp \int_0^\beta \mathrm{d}\tau \, \{-\epsilon_d(n_\uparrow + n_\downarrow) - U n_\uparrow n_\downarrow\} &= \mathrm{e}^{-\frac{U}{4}\int_0^\beta \mathrm{d}\tau \, \{(n_\uparrow+n_\downarrow)^2 + \frac{4}{U}\epsilon_d(n_\uparrow+n_\downarrow)\}} \mathrm{e}^{\frac{U}{4}\int \mathrm{d}\tau \, (n_\uparrow - n_\downarrow)^2} \\ &= \mathrm{e}^{\frac{\beta}{U}\epsilon_d^2} \delta(n_\uparrow + n_\downarrow + 2\epsilon_d/U) \mathrm{e}^{\frac{U}{4}\int_0^\beta \mathrm{d}\tau \, (n_\uparrow - n_\downarrow)^2}, \end{aligned} \tag{27}$$

where the delta function, which is defined by the last equality in the limit $U \to \infty$, implements the constraint of single-site occupancy in the symmetric case, $\epsilon_d = -U/2$.

The quartic interaction is decoupled by means of a Hubbard–Stratonovich boson field $X(\tau)$, according to the identity

$$\mathrm{e}^{\frac{U}{4}\int_0^\beta \mathrm{d}\tau \, (n_\uparrow - n_\downarrow)^2} = \int \mathrm{D}X \, \mathrm{e}^{-\frac{1}{4U}\int_0^\beta \mathrm{d}\tau \, (X^2(\tau) + 2U(n_\uparrow - n_\downarrow)X(\tau))}.$$

Now we have introduced the field $X(\tau)$, the partition function $\mathcal{Z}(\mu)$ takes the form

$$\begin{aligned} \mathcal{Z}(\mu) \propto \int \mathrm{D}X \, \mathrm{e}^{-\frac{1}{4U}\int_0^\beta \mathrm{d}\tau \, X^2(\tau)} \int \prod_i (\mathrm{D}d_i \, \mathrm{D}d_i^\dagger \, \mathrm{e}^{-\int_0^\beta \mathrm{d}\tau \, \mathrm{d}\tau' \, d_i^\dagger(\tau) G^{-1}_{(0)}(\tau - \tau') d_i(\tau')}) \\ \times \delta(n_\uparrow + n_\downarrow - 1) \tfrac{1}{2} \sum_{j=\uparrow,\downarrow} \mathrm{e}^{(-1)^j \int_0^\beta \mathrm{d}\tau \, [n_j - \frac{1}{2}] X(\tau)}. \end{aligned} \tag{28}$$

Note that now the term $\epsilon_d \sum_i n_i$ is included in equation (27), so in this case the dot Green function is $G^{-1}_{(0)}(\mathrm{i}\omega_n) = \mathrm{i}\omega_n - \Sigma_{(0)}(\mathrm{i}\omega_n)$. In contrast with the case $U = 0$, here the resonance is at the Fermi level, in spite of the fact that the original localized level is at ϵ_d. The partition function in equation (28) describes an effective spin 1/2 coupled to the fluctuating magnetic field $X(\tau)$; its dynamics is constrained by the requirement that the impurity is singly occupied. It could be shown that the single-site occupancy constraint is fulfilled on average when the partition function of equation (28) is used.

3.2. Quenching of the magnetic moment: the singlet ground state

The representation of the partition function given in equation (28) allows us to recognize the doubly degenerate ground state (GS) of the impurity spin $S_d = 1/2$ with $S^z_d = (-1)^\sigma (n_\sigma - 1/2)$, $\sigma = \uparrow, \downarrow$, driven by the field $X(\tau)$ and produced by virtual tunnelling of electrons on and off the dot at energy μ.

Anderson *et al* [21] calculated equation (28) by integrating out the impurity (d, $d^\dagger$ fields) and showing that the interaction with the delocalized electrons gives rise to a dynamics of the field $X(\tau)$ which also interacts with itself at different times according to a logarithmic law. The problem was solved by mapping equation (28) onto the partition function of a Coulomb gas (CG) [34] of flips in 1D, as we show in some detail in this subsection.

Let us define the new field $\xi(\tau) = X(\tau)/\Gamma$, where $\Gamma = \pi \nu(0)|V|^2$ is related to the tunnelling strength. At low temperatures, saddle point solutions of the resulting single-particle effective action are sequences of instantons $\xi_\pm(\tau, l) = \pm\xi_{\mathrm{M}} \tanh((\tau - \tau_l)/\tau_{\mathrm{M}})$ (where τ_l, $l = 1, 2, \ldots$ are the centres and $\tau_{\mathrm{M}} \sim \frac{1}{\epsilon_{\mathrm{F}}}$ is the width; that is, some cut-off which regularizes the theory at short times) corresponding to jumps between the two minima of the effective potential $V_{\mathrm{eff}}[\xi] = (\Gamma^2/U)\xi^2 - 2\Gamma/\pi[\xi \tan^{-1}(\xi) - \frac{1}{2}\ln(1+\xi^2)]$, located at $\xi_{\mathrm{M}} = \pm U/2\Gamma$, and interacting via a logarithmic potential $\alpha^2 \ln|(\tau_i - \tau_j)/\tau_{\mathrm{M}}|$.

For such a CG we can define the bare strength α^2_{b} of the logarithmic interaction (the 'charge') as $\alpha^2_{\mathrm{b}} = 2(1 - 8\Gamma/U\pi)$ and the 'fugacity' Y as $Y \equiv \tau_{\mathrm{M}} \mathrm{e}^{-S_{\mathrm{tot}}}$.

Thus, the full partition function may be approximated with the sum over the trajectories given by hopping paths and will be written as

$$Z = \sum_{N=0}^{\infty} \frac{1}{(2N)!} \int_0^\beta \frac{\mathrm{d}\tau_{2N}}{\tau_{\mathrm{M}}} \cdots \int_0^{\tau_2 - \tau_{\mathrm{M}}} \frac{\mathrm{d}\tau_1}{\tau_{\mathrm{M}}} \left[\mathrm{e}^{\frac{1}{2}\sum_{i\neq j=1}^{2N} (-1)^{i+j} \alpha^2 \ln\left|\frac{\tau_i - \tau_j}{\tau_{\mathrm{M}}}\right|} Y^{2N}\right]; \quad (29)$$

that is, the partition function of an effective one-dimensional gas of spin flips. The integral over the 'centres of the instantons' has to be understood such that τ_i and τ_j never become closer than τ_{M}.

Now, we are ready to perform the RG analysis to get the behaviour of the model at large timescales (low temperatures) [21]. The bare fugacity of the CG is $Y_{\mathrm{b}} = \tau_{\mathrm{M}} \exp(-\bar{\mathcal{A}})$ where $\bar{\mathcal{A}} \sim \tau_{\mathrm{M}} U$ is the action of one single flip. The scaling of the fugacity and the renormalization of the coupling constant induced by processes of fusion of charges lead to the following renormalization group (RG) equations [34]:

$$\frac{\mathrm{d}Y}{\mathrm{d}\ln\tau_{\mathrm{M}}} = \left(1 - \frac{\alpha^2}{2}\right) Y; \qquad \frac{\mathrm{d}\alpha^2}{\mathrm{d}\ln\tau_{\mathrm{M}}} = -2Y^2\alpha^2 \quad (30)$$

(see appendix A for a sketch of the derivation).

We see clearly that the flow is towards $Y \to \infty$ and $\alpha^2 \to 0$ and the scaling invariant energy (that is, the Kondo temperature which we will introduce in the next section) is $T_{\mathrm{K}} = \tau_{\mathrm{M}}^{-1} \mathrm{e}^{-1/(1-\frac{\alpha^2}{2})} \sim (U\Gamma)^{\frac{1}{2}} \mathrm{e}^{-\pi U/(8\Gamma)}$.

Condensation of instantons in the doubly degenerate GS leads to the Kondo singlet $\langle S^z\rangle = 0$ on the dot. Now we present a heuristic argument for such quenching of the total spin S on the dot; it runs as follows.

The dynamics of the field $\xi(\tau)$ with action $\bar{\mathcal{A}}$ can be mimicked by a two-level system Hamiltonian H_{2l} with hopping energy $\lambda \sim \frac{1}{2}m_{\rm eff}(\frac{{\rm d}\xi}{{\rm d}\tau})^2 \sim \frac{1}{2}\frac{\Gamma^2}{U}\tau_{\rm M}^2(\xi_{\rm M}/\tau_{\rm M})^2 \sim U/2$. The role of the interaction is to project out higher energy components from the dot states. Let us denote by $|\pm\rangle$ the two eigenstates of H_{2l}, i.e. the singlet and the triplet (with respect to the total spin of the dot plus conduction electrons, $S = 0$ and 1) on the dot. Instantons, by flipping the impurity spin, produce a dynamics of the system 'dot + conduction electrons' between these two states.

Now, let us make an interesting analogy with thermodynamics. At temperature β^{-1} the probabilities of having the system in one of the two states will be given by [35]

$$P_+ = \frac{1}{1+{\rm e}^{-2\beta\lambda}}; \qquad P_- = \frac{{\rm e}^{-2\beta\lambda}}{1+{\rm e}^{-2\beta\lambda}},$$

partly eliminating the component on the high energy eigenstate $|-\rangle$. Thus we are ready to give the connection with the CG picture described by the partition function of equation (29). In our case the dynamics is given by the coherent zero-point fluctuations of the system as a whole. From the statistical weight associated with a configuration with N instantons we can easily write down the formula

$$\langle N\rangle \equiv \langle N_{\rm inst}\rangle = \frac{\sum_{N=0}^{\infty} 2NY^{2N}/(2N)!}{\sum_{N=0}^{\infty} Y^{2N}/(2N)!} = Y\frac{\rm d}{{\rm d}Y}\ln(\cosh Y) = Y\tanh Y. \quad (31)$$

The frequency $\lambda/2\pi$ is obviously related to the average number of flips: $\beta\lambda/2\pi = \langle N\rangle = Y\tanh Y$, as a direct implication of equation (31).

Hence, the probabilities of having the system in the states $|\pm\rangle$ within the ground state ($T = 0$) are

$$P_+ = \frac{1}{1+{\rm e}^{-4\pi Y\tanh Y}}; \qquad P_- = \frac{{\rm e}^{-4\pi Y\tanh Y}}{1+{\rm e}^{-4\pi Y\tanh Y}}. \quad (32)$$

Because Y scales to infinity, the higher energy state completely decouples and the total spin on the dot is quenched: $\langle S^z\rangle \to 0$.

4. Perturbative analysis at $T \gg T_{\rm K}$

The Kondo effect in metals containing magnetic impurities is responsible for the 'anomalous' minimum in the resistivity $\rho(T)$, as the temperature $T \sim T_{\rm K}$: such a minimum in $\rho(T)$ is due to scattering of conduction electrons off the localized magnetic impurities. Those contributions were first worked out by Kondo [36], who derived a correction $\Delta\rho(T) \propto \ln(\frac{T_{\rm K}}{T})$.

As we pointed out in the introduction, a different realization of the Kondo effect may be achieved, in a controlled way, in a quantum dot in the Coulomb blockade (CB) regime [3]. The Kondo effect in a dot is usually detected by measuring the linear conductance as a function of the gate voltage by connecting two electrodes to the dot. A dot at CB exhibits discrete energy levels. Changing the number of electrons is strongly prevented by electrostatic charging energy. Correspondingly, the total charge at the dot is quantized and the linear conductance is zero within large windows of variations of the gate voltage ('CB valleys'). By analysing the level structure of the dot it has been shown that, in some special cases, the dot at CB behaves as a magnetic moment antiferromagnetically interacting with the magnetic momenta of lead electrons. CB valleys at different occupation number of the dot are bounded by resonant conduction peaks, as the chemical potential of the leads matches that of the dot. Those peaks usually get sharper and better defined as T is lowered. However, as $T \sim T_{\rm K}$, the Kondo effect

arises at the dot. Consequently, the CB valley between two resonant conduction peaks 'fills in' in a way that does not depend on the position of the Fermi level of the leads [3]. As $T \sim T_{\rm K}$, the conductance $g(T)$ exhibits the typical logarithmic rise [37]. The logarithmic rise, however, cannot hold all the way down to $T = 0$, as it must be limited by the unitarity bound. Therefore, a different approach is required in order to study the Kondo effect in the $T = 0$ unitarity limit, as we will discuss in the next section.

In this section we derive the Kondo Hamiltonian from the single-impurity Anderson model (equation (22)) focusing for simplicity on the isotropic case $J_\perp = J_z = J$; then we sketch the perturbative renormalization group (RG) flow for the coupling strength of such a model. In general, the lower T, the more spin flip processes become likely, which makes the running coupling constant J grow. At the Kondo temperature $T_{\rm K}$ the perturbative analysis breaks down; that is, $\nu(0)J(T_{\rm K}) \sim 1$, so $T_{\rm K}$ is the characteristic scale that divides the regions of weak and strong coupling.

4.1. Derivation of the spin dynamics Hamiltonian

In the following we will restrict our analysis to a twofold-degenerate dot level: in such a case the QD can be modelled as a spin $1/2$ magnetic impurity. Indeed, because the charge degree of freedom is frozen at the Coulomb blockade we mimic the dot with its total spin $\vec{S}_d$ and describe its interaction with the delocalized electrons by means of the Kondo Hamiltonian:

$$H_{\rm eff} = H_{\rm lead} + H_{\rm K} \equiv H_{\rm lead} - J\vec{S}_d \cdot \vec{\sigma}(0), \tag{33}$$

where $\vec{\sigma}(0) = \sum_{kk'} \sum_{\sigma\sigma'} (c^\dagger_{k\sigma} \vec{\tau}_{\sigma\sigma'} c_{k'\sigma'})$ plays the role of a spin density of the itinerant electrons at the impurity site ($\vec{\tau}_{\sigma\sigma'}$ are the Pauli spin $1/2$ matrices). Its components each behave as a spin $1/2$, provided that single occupancy of the site $x = 0$ is guaranteed.

In the anisotropic Kondo model the couplings of the x, y components $J_\perp$ are different from that of the z component J_z. This effective Hamiltonian is more suitable for describing the low T physics of the system because its dynamics shows how the system flows towards the non-perturbative regime. In the following sections, by 'low temperature' we will mean $T \sim T_{\rm K}$.

As a first step we show that it is possible to derive the effective Hamiltonian (33) from the one for the single-impurity Anderson model (equation (22)), where $H_{\rm D} = \epsilon_d \sum_\sigma n_\sigma + U \sum_{\sigma\sigma'} n_\sigma n_{\sigma'}$, by means of the Schrieffer–Wolff (SW) transformation [38]. More details can be found in the book by Hewson [5].

Let Ξ be the space spanned by the (almost) degenerate dot states. As the number of electrons at the QD is fixed, the relevant degrees of freedom can be described by an effective Hamiltonian $H_{\rm eff}$ acting on Ξ only. In order to construct $H_{\rm eff}$, we apply the SW transformation to the Hamiltonian in equation (22). We denote by P the projector onto Ξ and by ϵ_d the energy of the states within Ξ, so the effective Kondo Hamiltonian is given by

$$\delta H_{\rm eff} \approx PV(1-P)\frac{1}{\epsilon_d - H_{\rm D} - H_{\rm lead}}(1-P)VP. \tag{34}$$

Indeed, by inserting equation (22) into (34), we get the result

$$\begin{aligned} H_{\rm eff} = H_{\rm lead} &- \nu(0)\sum_{\alpha\sigma}\frac{V_\alpha^2}{\epsilon_d} d^\dagger_\sigma d_\sigma + \sum_{\alpha\sigma;k,k'} V_\alpha^2 \left[\frac{1}{\epsilon_d + U} + \frac{1}{\epsilon_d}\right] c^\dagger_{k\alpha\sigma} c_{k'\alpha\sigma} \\ &- \sum_{\alpha,\alpha';\sigma,\sigma';k,k'} V_\alpha V_{\alpha'} \left[\frac{1}{\epsilon_d + U} - \frac{1}{\epsilon_d}\right] c^\dagger_{k\alpha\sigma} \vec{S}_d \cdot \vec{\tau}_{\sigma\sigma'} c_{k'\alpha'\sigma'} \end{aligned} \tag{35}$$

where $S^z_d = \sum_\sigma \sigma d^\dagger_\sigma d_\sigma$, $S^+_d = d^\dagger_\uparrow d_\downarrow$ and $S^-_d = d^\dagger_\downarrow d_\uparrow$ are the impurity spin components. Spin commutation relations are obtained if no double occupancy is admitted.

Besides $H_{\rm lead}$, the first and the second term on the rhs of equation (35) represent, respectively, a renormalization of the dot's energies and a potential scattering term; the third term is the one which induces spin flips. The two contributions appearing in the potential scattering term and in the spin flip term refer to two virtual particle and hole processes, respectively. In the first case a particle is added to the dot so that the energy $\epsilon_d + U$ is involved, while in the second case a particle is subtracted from the dot level, thus paying the energy $|\epsilon_d|$. The potential scattering term vanishes if the Anderson model is symmetric, as we have assumed up to now ($\epsilon_d = -U/2$).

4.2. The perturbative renormalization group approach

In this subsection the starting point of our reasoning is, for simplicity, the isotropic limit of the Kondo Hamiltonian in equation (33). The scattering of conduction electrons by the impurity produces a self-energy correction, as well as a correction to the interaction vertex. The transitions between the states close to the Fermi level $\epsilon_{\rm F}$ and the states within a narrow strip of energies of width δD near the edges of the band of width $2D$ are associated with a high energy deficit. Such transitions are virtual and their influence on the states near $\epsilon_{\rm F}$ can be taken into account perturbatively in second order. In the *poor man's scaling* approach one includes second-order corrections arising from processes in which the electrons k' are scattered to an intermediate state at energy $D > \epsilon_{k''} > D - \delta D$ or $-D < \epsilon_{k''} < -D + \delta D$ where D is some ultraviolet cut-off. Because they involve high intermediate energies, one can think of including them perturbatively; so for an electron k' scattered into the final state k we have

$$\sum_{k''\in\gamma} \langle k|H_{\rm K}|k''\rangle\langle k''|\frac{1}{E - H_{\rm lead}}|k''\rangle\langle k''|H_{\rm K}|k'\rangle \sim -J^2\nu(0)\delta D\frac{1}{D}\vec{S}_d \cdot \sum_{kk'}\sum_{\sigma\sigma'} c^{\dagger}_{k\sigma}\vec{\tau}_{\sigma\sigma'}c_{k'\sigma'} \qquad (36)$$

where γ is the k'' domain mentioned above. To justify the second step one observes that, in the shell γ, the operator $H_{\rm lead}$ can be replaced by an energy D and, in comparison to it, the eigenvalue E can be put at the Fermi level $E = 0$. The result is an effective Hamiltonian acting within the band of a reduced width $D - \delta D$, of the same form as $H_{\rm K}$ in equation (33) but with a modified value of J. This gives the following correction to the previous coupling constant in $H_{\rm K}$: $\delta J \sim -J^2\nu(0)\delta D/D$ [39]. Successive reductions of the bandwidth by small steps δD can be viewed as a continuous process during which the initial Hamiltonian is transformed to an effective low energy Hamiltonian acting within the band of reduced width $D - \delta D$. The evolution of the exchange amplitude J during such a *poor man's scaling* can be cast in the form of a flow differential equation [39]:

$$\frac{{\rm d}J}{{\rm d}\ln D} = -\nu(0)J^2. \qquad (37)$$

Integration of equation (37) gives rise to the renormalization of J:

$$\frac{1}{j(D)} - \frac{1}{j(D_0)} = \ln\frac{D}{D_0}, \qquad (38)$$

where $j = J\nu(0)$; that is,

$$j(D) = \frac{j_0}{1 - j_0\ln\frac{D_0}{D}}. \qquad (39)$$

Scaling can be performed down to $D \sim k_{\rm B}T$; also we see that, if $j_0 \equiv j(D_0) > 0$ (antiferromagnetic coupling), the running coupling constant j increases. Equation (38) shows that $D{\rm e}^{-1/j}$ is a constant of this flow, which defines an energy scale $T_{\rm K}$:

$$k_{\rm B}T_{\rm K} = D_0{\rm e}^{-1/j_0}. \qquad (40)$$

In general, at the Kondo temperature T_K the system has approached the scale at which the perturbative analysis breaks down, so for $T < T_K$, j starts to diverge in the flow.

Now we discuss the conductance in such a perturbative limit. Let us take a $\delta(x)$-like dot with an even barrier potential ($\Gamma_R = \Gamma_L$). To lowest perturbative order the leading self-energy correction to $t^0(\omega + i0^+)$ (see equations (16), (17)) ($\omega = 0$) yields

$$g = \left|\frac{\pi}{k_0}t^0\right|^2 = \mathrm{Re}\left\{\frac{i\pi}{k_0}t^0\right\} \approx \pi^2(\nu(0)J)^2, \tag{41}$$

where $\frac{1}{\nu(0)J} = \ln\frac{T}{T_K}$ is the invariant charge defined through equation (40), so the conductance can be written as

$$g \approx \pi^2 \ln^{-2}\frac{T}{T_K}, \qquad T_K \ll T \ll D. \tag{42}$$

The tail of the conductance in the perturbative limit $T \gg T_K$ is logarithmic.

4.3. The one-channel anisotropic Kondo model and the Toulouse limit

In the following we rewrite the Coulomb gas approach introduced in section 3.2 focusing on the single-channel anisotropic Kondo system. Let us start from the general effective Hamiltonian:

$$H_{\mathrm{eff}}^{A} = H_{\mathrm{lead}} + H_K^A \equiv H_{\mathrm{lead}} + J_z S_d^z \sigma_z(0) + \frac{J_\perp}{2}(S_d^+\sigma_-(0) + S_d^-\sigma_+(0)). \tag{43}$$

As stated in [21], the perturbation term (the one containing $J_\perp$) has the effect of flipping the local spin at each application; hence the problem of calculating the partition function of such a system reduces to the evaluation of the amplitude for a succession of spin flips at times $\tau_1, \tau_2, \ldots$ and the Feynman sum over histories is the sum over all possible numbers and positions of flips. So, we get the expression (29) which can be rewritten as

$$Z_{CG} = \sum_{N=0}^{\infty}(J_\perp\tau_M)^{2N}\int_0^\beta \frac{d\tau_{2N}}{\tau_M}\cdots\int_0^{\tau_2-\tau_M}\frac{d\tau_1}{\tau_M}\left[e^{+\sum_{i\neq j=1}^{2N}(-1)^{i+j}(2-\varepsilon)\ln\left|\frac{\tau_i-\tau_j}{\tau_M}\right|}\right]. \tag{44}$$

Here ε is the quantity

$$\varepsilon = \frac{8\delta_{AF}}{\pi} - \frac{8\delta_{AF}^2}{\pi^2} \simeq 2J_z\tau_M \tag{45}$$

where δ_{AF} is the scattering phase shift of the antiferromagnetic sign introduced by the $J_z S_d^z\sigma_z(0)$ term. It can be seen clearly that the sign of J_z, or ε, determines whether the coupling is ferromagnetic or antiferromagnetic, so the condition $\varepsilon > 0$ gives the antiferromagnetic coupling.

Let us now notice that equation (44) is a function of three parameters only: $\frac{\tau}{\tau_M}$, $J_\perp\tau_M$, ε; we are interested to the case $\tau \to \infty$ (low temperature). In such a case it is well known that the ferromagnetic Kondo system has a mean spin moment which corresponds to a long range order of the classical system: the positive and negative charges are all bound in pairs forming dipoles all pointing in the same direction. The phase transition occurs, at least for small $J_\perp$, at the ferromagnetic–antiferromagnetic boundary point $\varepsilon = 0$.

For such a system it is possible to derive a set of scaling laws that are exact for small $J_\perp\tau_M$ and ε. The physical picture is that of many close pairs of flips which slightly change the mean magnetization, located between pairs of isolated flips which are reversals of the magnetization over a larger timescale; so, the isolated flips can be considered as acting in a medium where the close pairs modify the mean magnetization. This line of reasoning leads to the following scaling laws for the 'fugacity' $J_\perp\tau_M$ and the 'charge' ε respectively:

$$\frac{d(J_\perp\tau_M)}{d\ln\tau_M} = \frac{\varepsilon}{2}(J_\perp\tau_M); \qquad \frac{d\varepsilon}{d\ln\tau_M} = (2-\varepsilon)(J_\perp\tau_M)^2. \tag{46}$$

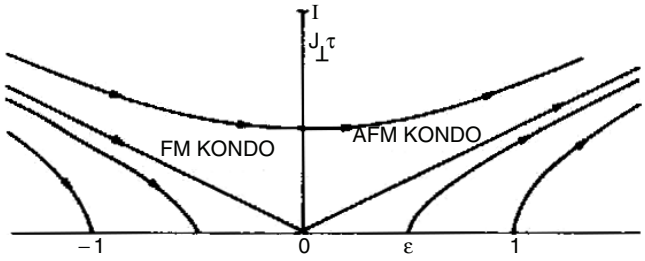

Figure 3. The renormalization group flow diagram for small J [21].

Let us make a few comments on such equations. First, these are also exact for finite ε, because only $J_\perp \tau_M$ need to be small. Second, they are compatible in the isotropic case $J_z = J_\perp$, $\varepsilon \simeq 2J_z\tau_M \simeq 2J_\perp\tau_M$ where $J_\perp\tau_M$ and ε are small; because $J_\perp\tau_M$ and ε scale together, the isotropic Kondo system remains isotropic at every timescale. In the anisotropic model, equations (46) become:

$$\frac{d\varepsilon}{d(J_\perp\tau_M)} \simeq 4\frac{J_\perp\tau_M}{\varepsilon}; \qquad \varepsilon^2 - 4J_\perp^2\tau_M^2 = \text{constant}; \tag{47}$$

thus the scaling lines are a set of hyperbolas with asymptotes corresponding to the isotropic case.

We see clearly from figure 3 that all ferromagnetic cases below the isotropic one scale onto the case $J_\perp\tau_M = 0$ which is an ordered one, so the transition line coincides with the ferromagnetic case. Conversely, in the antiferromagnetic (AF) case $J_\perp\tau_M$ and ε increase starting from certain values, small at will, and we can always find a timescale for which $\varepsilon \sim 1$. Such a timescale is a crucial one for the Kondo phenomenon; it is the Kondo temperature already introduced in the previous sections and sets the scale at which the system behaves as if it were strongly coupled. Thus, the renormalization procedure is valid up to $\varepsilon \sim 1$.

Now, let us briefly focus on the so-called Toulouse limit $J_z = J_\perp$, $\varepsilon \sim 1$; in such a case the system is equivalent to a simple quadratic model with the Hamiltonian

$$H_T = \sum_k \epsilon_k c_k^\dagger c_k + V\sum_k [d^\dagger c_k + c_k^\dagger d]. \tag{48}$$

Here c_k, $c_k^\dagger$ are Fermi operators for free spinless electrons and d, $d^\dagger$ are Fermi operators for a local resonant state. The partition function corresponding to the Hamiltonian (48) is exactly equal to the one in equation (44) for the case of classical charges ± 1. Such a theory corresponds to free particles and there is no renormalization.

5. Breakdown of the perturbative approach at $T \sim T_K$: the strong coupling fixed point

In the previous section we have derived the perturbative flow equation for the Kondo coupling constant J. Integration of the renormalization group (RG) equation shows that J grows as T is lowered, until the perturbative analysis does not make any sense any longer. The question of whether the RG flow stops at some finite T scale fixed coupling or goes all the way down to $T = 0$ has been widely debated in the literature (see [5] for a review on the subject). However, from numerical RG analysis and from the exact Bethe ansatz solution of the model [7] it is now clear that the system takes no fixed points at finite T, but the RG flow goes all the way down to $T = 0$. So, the aim of this section is to discuss the physics of the Kondo system in the $T = 0$ unitarity limit.

In the case of a localized spin $1/2$ impurity antiferromagnetically interacting with the spin of one type of itinerant electron only (the spin $1/2$ one-channel Kondo effect), the theory of the unitary limit was first developed by Noziéres [40]. As T is lowered all the way down to 0, the flow of the coupling strength runs all the way toward an infinite coupling fixed point. At the fixed point, the impurity spin is fully screened and the localized magnetic moment is effectively replaced by a spinless potential scattering centre with infinite strength (which forbids double occupancy at the impurity site). The $T \to 0$ 'unitarity limit' is well described by a Fermi liquid theory, which also allows for calculation of finite T corrections to fixed point values of the physical quantities. Both elastic and inelastic scattering processes provide finite T contributions to the conductance. As we will show in the next section, the two kinds of process contribute at the same order, thus giving rise to corrections to the unitary limit proportional to $(\frac{T}{T_K})^2$ [40].

A generalization of Kondo's original idea was carried out by Noziéres and Blandin [41]. They showed that the interaction of itinerant electrons with magnetic impurities in metals may involve electrons with different quantum numbers besides the spin: for instance, electrons with different orbital angular momentum. Different orbital quantum numbers define different 'channels' of interaction. Therefore, a 'many-channel' Kondo effect may arise. Although in the perturbative region there is no qualitative difference between one-channel and many-channel effects, deep differences may arise in the unitarity limit, depending on the number of channels K and on the total spin of the impurity, S.

In the case $2S = K$, at $T = 0$ the magnetic moment at the impurity is fully screened by electrons from the leads. The impurity forms a singlet state with $2S$ conduction electrons and no other electrons can access the impurity site. The system behaves exactly as if there were no impurity, besides a boundary condition on the wavefunction of conduction electrons which takes into account that the impurity site is 'forbidden' to them [40]. Such a Fermi liquid state is stable against leading finite T corrections, as we shall see below, and corresponds to an infinite effective coupling $\nu(0)J$. A special case of this is the one-channel Kondo effect just discussed, with $S = \frac{1}{2}$ and $K = 1$.

In the case $2S > K$, in the strong coupling regime a residual magnetic moment is still present at the impurity, since there are no more conduction electrons able to screen the localized spin. The corresponding fixed point is again a Fermi liquid, but with a localized partially screened magnetic moment at the impurity that is *ferromagnetically* coupled to the itinerant electrons: it again provides the stability of the local Fermi liquid.

A very special case is the $2S < K$ one. In such a case conduction electrons attempt to 'overscreen' the impurity in the strong coupling limit; that is, the resulting magnetic moment is opposite to the original one. The coupling among the localized residual magnetic moment and the itinerant electrons is now *antiferromagnetic*. It drives the system out of the strongly coupled regime towards a finite coupling fixed point J_* [41], as we clearly see in figure 4. At $J = J_*$ the leading finite T interaction is given by a marginal three-particle operator which breaks down the Fermi liquid state and generates a non-Fermi liquid behaviour in the physical quantities. We will discuss such an issue in section 7 of this review.

6. The fully screened single-channel Kondo case

6.1. Finite temperature corrections to the one-channel Kondo conductance

At $T = 0$ the linear response of the Kondo system to an applied voltage bias reaches the so-called unitarity limit.

The response function is the resistivity in a bulk system (magnetic impurities in dilute alloys), while it is the conductance in a quasi-one-dimensional system such as the system that we are interested in: a dot with applied contacts.

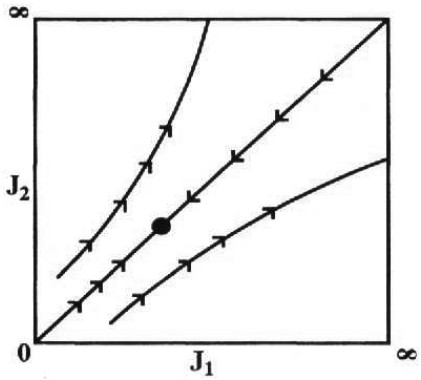

Figure 4. A qualitative renormalization group flow diagram for the anisotropic two-channel Kondo problem; the non-trivial fixed point corresponds to $J_1 = J_2 = J_*$ (channel symmetry) [42].

The striking feature of the Kondo effect in dilute alloys is the minimum in the resistivity at low temperature which violates the expected property: $d\rho/dT > 0$. Indeed, well below T_K the resistivity increases again up to a maximum value proportional to the number of impurities N_i per unit volume (the 'unitarity limit').

In contrast, a maximum of the conductance is expected at $T = 0$ for Kondo conductance across a quantum dot, where the unitarity limit that is reached is $\frac{2e^2}{h} g_u$.

Since the s-wave scattering is effectively one-dimensional-like, such a 'reversed behaviour' looks paradoxical. However, it is just a consequence of the difference between the 3D and 1D impurity scattering, as we explain here. In order to illustrate the difference, it is enough to note that both facts stem from the main feature of Kondo impurity scattering: the formation of a resonance at the Fermi level due to many-body effects, which implies that the phase shift reaches the value $\delta = \pi/2$ and that scattering is resonant at the impurity. This produces different results in the two cases:

3D: a spherical s wave is diffracted from the impurity with maximum amplitude at resonance, which increases the flux propagating backward and enhances resistivity;

1D: resonant scattering coincides with resonant transmission in this case, which implies the vanishing of backward reflection and enhances the conductance.

Temperature corrections are twofold. One is due to the energy dependence of the phase shift close to the resonance $\delta^0(\epsilon) = \pi/2 - a\epsilon^2$ and to the fact that energies close to the Fermi surface are sampled, because the Fermi functions are not step-like at finite T. The second one is due to inelastic processes which produce transitions from the singlet ground state to the excited states. The latter can be accounted for with an expansion in inverse powers of the singlet binding energy [40]. We include a simplified approach to the problem which rests on the Fermi liquid nature of the excitation spectrum in appendix B [40, 8, 10]. It is found that corrections to the conductance are quadratic in temperature, as is usual in the Fermi liquid theory:

$$g = g_u\left[1 - \left(\frac{\pi T}{T_K}\right)^2\right], \qquad T \ll T_K. \tag{49}$$

The weak coupling ($T \gg T_K$) and the strong coupling ($T \ll T_K$) asymptotes of the conductance, equations (42) and (16), have very different structures but, since the Kondo

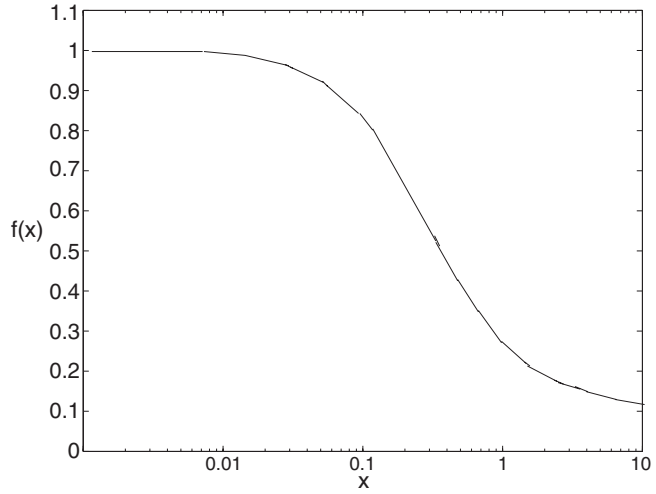

Figure 5. A plot of the universal function $f(x)$ versus $x = T/T_K$ [11].

effect is a crossover phenomenon rather than a phase transition [6, 7], the dependence $g(T)$ is a smooth function [10] throughout the crossover region $T \sim T_K$:

$$g = g_u f\left(\frac{T}{T_K}\right). \tag{50}$$

The universal function $f(x)$, as is found by resorting to the numerical renormalization group (NRG) in [10, 11], is plotted in figure 5. It interpolates between $f(x \gg 1) = \frac{3\pi^2}{16}(\ln x)^{-2}$ and $f(0) = 1$.

6.2. The Kondo resonance in a magnetic field

A small magnetic field B lifts the degeneracy of the spin states at the impurity. This produces a splitting of the resonance and a change of its shape which has been numerically studied mostly via the NRG [11]. The splitting of the peak increases linearly with B and is $\Delta = 2\mu_B B$, i.e. twice the Zeeman spin splitting.

This can be understood easily if one considers the particle and hole virtual occupations which mediate the Kondo interaction.

Let us consider the symmetric case $\epsilon_d = -U/2$. The dot states with N electrons and one unpaired spin are $N\uparrow$ and $N\downarrow$ corresponding to $\epsilon_d + B/2$ ($\mu_B = 1$) and $\epsilon_d - B/2$, respectively. In the presence of spin splitting two particle processes are allowed: p_σ ($p_{-\sigma}$) in which a spin $-\sigma$ is added to the state $N\sigma$ and subsequently a spin $-\sigma$ is removed with the energy balance

$$p_\downarrow \to \delta E(N\uparrow, +\downarrow) + \delta E(N+1, -\uparrow) = U + (-U - B) = -B,$$
$$p_\uparrow \to \delta E(N\downarrow, +\uparrow) + \delta E(N+1, -\downarrow) = (U + B) + (-U) = B.$$

Similarly the hole processes have an energy balance

$$h_\uparrow \to \delta E(N\uparrow, -\uparrow) + \delta E(N-1, +\downarrow) = (-\epsilon_d - B/2) + (\epsilon_d - B/2) = -B,$$
$$h_\downarrow \to \delta E(N\downarrow, -\downarrow) + \delta E(N-1, +\uparrow) = (-\epsilon_d + B/2) + (\epsilon_d + B/2) = B.$$

This implies that there are two peaks in the spectral density at $\omega = \pm B$ corresponding to the $p_\downarrow, h_\uparrow$ and $p_\uparrow, h_\downarrow$ spin flip processes, respectively.

The value at the Fermi energy of the spectral function is related to the B dependent phase shift in the Fermi liquid picture by the Friedel sum rule:

$$-\pi\nu(0)\,\mathrm{Im}(t_\sigma(\omega=0,T=0,B))=\sin^2\delta_\sigma(B). \tag{51}$$

The Bethe ansatz solution of the problem relates the phase shift at the Fermi level to the magnetization of the impurity: $\delta_\sigma(B)=\frac{\pi}{2}[1-2M_d(B)]$ [43]. Hence a reduction of the peak height with increase of the magnetic field follows.

It has also been argued that the renormalizability of the Kondo problem could break down when B exceeds some critical value related to the Kondo temperature, because of the back action of the induced conduction electron polarization cloud on the impurity leading to a broken symmetry state with $\langle S_z\rangle\neq 0$ [44].

6.3. Crossing of the dot levels in a magnetic field and enhancement of the Kondo conductance

Conventional Kondo resonant transmission requires a magnetic moment to be present on the dot. Usually dots with an even number of electrons are in a singlet state, while dots with an odd number of electrons have an unpaired spin and have a doublet GS. Hence, there is a parity effect: CB conduction valleys with $N=$ even do not display the Kondo conductance while those with $N=$ odd do. An exception to this rule occurs at zero magnetic field when Hund's rule applies. This was found experimentally in the vertical QD, e.g. at $N=6$. The GS of the isolated dot has $S=1$ (triplet) [45]. An underscreened Kondo effect is expected at this point and the GS of the interacting system becomes a doublet. By applying a weak magnetic field orthogonal to the dot ($B=0.22$ T), a transition of the GS from triplet to singlet (T–S) has been found. The single-particle energy levels become angular momentum dependent and Hund's rule no longer applies. Close to the crossing a remarkable enhancement of the Kondo coupling with increase of the Kondo temperature was found experimentally. Indeed, scaling shows a non-universal critical temperature when the interplay of the fourfold-degenerate states ($|SS_z\rangle$ with $S=0,1$) is included [46].

An extended and unified approach to the problem can be found in [47]. A minor difference is the fact that they consider an in-plane magnetic field as the source of the crossing which could produce Zeeman spin splitting (ZSS) of the single-particle states. The four dot states are mapped onto a two-impurity Kondo model (2IKM) [48] with spin $\vec{S}_1,\vec{S}_2$. However, they are coupled by a potential term $Vn\rho_{nn}(0)\vec{S}_1\cdot\vec{S}_2$ and an exchange term $\mathrm{i}Ins_{\overline{n}n}(0)\vec{S}_1\times\vec{S}_2$. Here ρ,σ are the charge and spin density of the conduction electrons with n and $\overline{n}\neq n$ labelling two different orbital states. Because these terms violate the invariance under particle–hole transformation, the 2IKM cannot flow by scaling to the non-Fermi liquid fixed point, which is known to be a remarkable feature of the model. In the case of large ZSS Δ, the RG flow terminates at $D\approx\Delta$. Two of the four states are ruled out in the flow and conduction electrons couple to one single effective spin $1/2$ with one extra unusual term in the effective Hamiltonian which is a Zeeman term for the conduction electrons.

Kondo conductance can take place in a dot with an even number of electrons also in a strong vertical magnetic field [35]. Orbital effects induced by B can produce the reversed transition from the singlet to the triplet state (S–T). Indeed, a vertical magnetic field on an isolated dot favours transitions to higher spin states [49]. In this case the ZSS is anyway sizable and the crossing involves the singlet state and the component of the triplet state lowest lying in energy. In a vertical geometry with cylindrical symmetry, the orbital angular momentum m and z spin component σ are good quantum numbers. In particular, because the singlet state has total angular momentum $M=0$ and the triplet state involved in the crossing has $M=1$, only a ($m=0\downarrow$) electron can enter the dot when it is in the triplet state. In contrast, only an

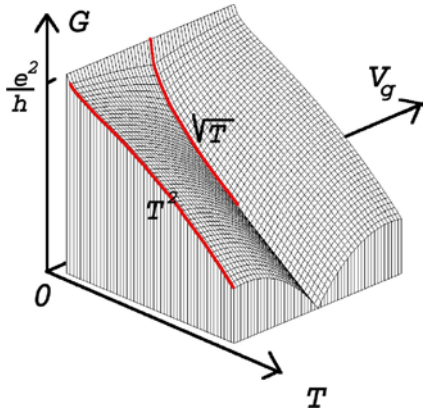

Figure 6. A sketch of the conductance across the dot as a function of the temperature T and the gate voltage V_g [24].

($m = 1\uparrow$) electron can enter the dot, if it is in the singlet state. This implies that there is one single channel of conduction electrons involved in cotunnelling processes, with orbital and spin degrees of freedom locked together. Again, a residual effective spin 1/2 survives at the dot, while N is even [23]. This is another striking manifestation of the spin–charge separation that occurs at the Kondo fixed point. Usual Kondo coupling leads to $N =$ odd together with $S = 0$. In the complementary situation here described, it is $N =$ even and $S = 1/2$.

7. The overscreened two-channel Kondo case

A two-channel Kondo behaviour has been invoked in an experiment by Ralph and Buhrman [50] on clean Cu point contacts, defects in the metal that can be described by two-level systems (TLS). The TLS could tunnel between the even and odd states with the assistance of the conduction electrons. Their physical spin is not involved in the scattering, so two channels are available [51]. It is still unclear whether the Kondo temperature can be large enough that any effect of the Kondo correlation can be measured [52]. However, these experiments have triggered renewed interest in two-channel Kondo conductance. The temperature and voltage dependence of the conductivity have been numerically calculated within the 'non-crossing approximation' (NCA) [53] and found to be consistent with a scaling ansatz motivated by the conformal field theory (CFT) solution of the problem [8]. Since then, no other experimental proof of two-channel Kondo effect in impurities has been produced. The result for the imaginary part of the transmission t is

$$\operatorname{Im} t(\omega) \sim \sqrt{\frac{\omega}{T_K}}. \tag{52}$$

From this result, we get a $\sqrt{T/T_K}$ temperature dependence of the conductance as $T \to 0$, which is a clear signature of the breakdown of the Fermi liquid [8] (see figure 6).

In order to emphasize the deep difference between single-channel and many-channel Kondo effect in the $T = 0$ limit we just mention here that the imaginary part of the proper self-energy, close to the Fermi surface, behaves as $\operatorname{Im}\Sigma(k,\omega) \propto C_k\omega^2$ (where the chemical potential $\mu = 0$ is taken as the reference energy) in the Fermi liquid case and in the single-channel Kondo problem. In contrast, it behaves as $\operatorname{Im}\Sigma(k,\omega) \propto C'_k\omega^{\frac{1}{2}}$ in the two-channel

'overscreened' Kondo problem. In the following we refer, for simplicity, to the two-channel 'overscreened' case. Through the Kramers–Kronig relation

$$\frac{\partial}{\partial\omega}\,\mathrm{Re}\,\Sigma(k,\omega) = -\frac{1}{\pi}P\int_{-\infty}^{\infty}\mathrm{d}\omega'\,\frac{\partial_\omega\,\mathrm{Im}\,\Sigma(k,\omega')}{\omega'-\omega} \tag{53}$$

we see that $\frac{\partial}{\partial\omega}\,\mathrm{Re}\,\Sigma(k,\omega)|_{\omega\to 0}$ is finite in the first case, at the Fermi surface; in contrast it has a power law divergence in the second case. It follows that the quasiparticle pole residue $z_k = [1-\partial_\omega\Sigma(k,\omega)]^{-1}|_{\omega\to 0}$ vanishes as a power law in the second case at the Fermi surface. Luttinger [54] showed that, to all orders of perturbation theory in the interaction, the imaginary part of the proper self-energy behaves as $\mathrm{Im}\,\Sigma(k,\omega)\propto C_k\omega^2$ ($C_k>0$) close to the Fermi surface, which implies an infinite lifetime for the quasiparticles at the Fermi surface. The Fermi surface is sharp and well defined. These are the foundation stones of the normal Fermi liquid theory and they are invalidated in the spin $1/2$ two-channel Kondo case.

In this section we focus, in particular, on the two-channel spin $1/2$ Kondo effect in both the perturbative region and the unitarity limit. We describe the scaling perturbative approach and the bosonization ($T\sim 0$) technique, respectively. An attempt to extend the Anderson–Yuval approach of section 4.3 to the two-channel Kondo case can be found in [42].

7.1. Perturbative analysis at $T \gg T_{\mathrm{K}}$

The starting point of our reasoning is the effective Hamiltonian given in equation (35), which we will take in the isotropic limit. In the following we will restrict our analysis to a twofold-degenerate dot level. In this case, as we pointed out, the QD can be modelled as a spin $1/2$ magnetic impurity, whose spin is given by

$$S_d^a = \tfrac{1}{2}d_\gamma^\dagger\tau^a_{\gamma\gamma'}d_{\gamma'}$$

(that $\vec{S}_d$ is a spin $1/2$ comes out from the identity $\vec{S}_d^2 = 3/4$, valid in the case of single occupancy for the dot's level).

In this case and for a generic number of channels for the itinerant electrons, equation (35) takes the form

$$H_{\mathrm{K}} = J\sum_a\left(\sum_{\gamma\gamma'}\left(d_\gamma^\dagger\frac{\tau^a_{\gamma\gamma'}}{2}d_{\gamma'}\right)\sum_{kk'}\sum_{\sigma\sigma';\alpha}\left(c^\dagger_{k\sigma\alpha}\frac{\tau^a_{\sigma\sigma'}}{2}c_{k'\sigma'\alpha}\right)\right) \tag{54}$$

where $\alpha\in(1,\ldots,K)$ is the channel index and the constant J is taken as a perturbative parameter (>0). Infrared divergent diagrams provide a flow of J as a function of T. We are now going to derive the perturbative β function at third order in J. At finite T the Green function in Fourier space will depend on the momentum of the particles and on the Matsubara frequencies $\omega_m = \frac{2\pi}{\beta}(m+\frac{1}{2})$ (for fermions). In our case, the Green function for the lead electrons is given by

$$G_{\sigma\sigma';\alpha\alpha'}(\mathrm{i}\omega_m,k) = \mathbf{FT}\{\langle\hat{T}[c_{\sigma\alpha}(\tau,k)c^\dagger_{\sigma'\alpha'}(0,k)]\rangle\} = \frac{\delta_{\sigma\sigma'}\delta_{\alpha\alpha'}}{\mathrm{i}\omega_m - v_{\mathrm{F}}k} \tag{55}$$

where **FT** stands for 'Fourier transform' and $\hat{T}$ is the time ordering operator, while the Green function for the d fermion is

$$\mathcal{G}_{\gamma\gamma'}(\mathrm{i}\omega_m) = \mathbf{FT}\{\langle\hat{T}[d_\gamma(\tau)d^\dagger_{\gamma'}(0)]\rangle\} = \frac{\delta_{\gamma\gamma'}}{\mathrm{i}\omega_m}. \tag{56}$$

The interaction vertex determined by H_{eff} is

$$V^{\alpha\alpha'}_{\sigma\sigma';\gamma\gamma'}(\{\mathrm{i}\omega_m^{(j)}\}) = \delta_{\alpha\alpha'}\frac{J}{4}\tau^a_{\gamma\gamma'}\tau^a_{\sigma\sigma'}\delta(\omega_m^{(1)}+\omega_m^{(2)}-\omega_m^{(3)}-\omega_m^{(4)}). \tag{57}$$

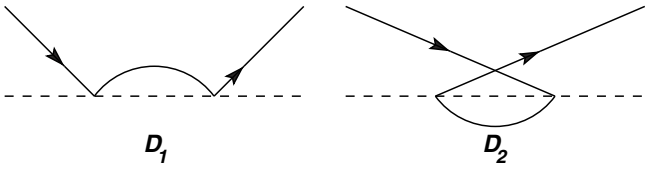

Figure 7. Second-order diagrams $\mathcal{D}_1$ and $\mathcal{D}_2$. Conduction fermions are represented as full lines, while dashed lines represent the propagation of d fermions (dot states).

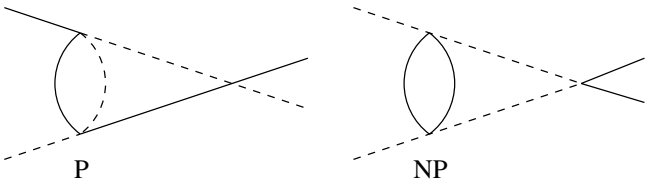

Figure 8. Third-order vertex renormalization. The first case (P) is a 'parquet-type' diagram. Its contribution is accounted for in the integration of the second-order RG equation. The second one (NP) is a 'non-parquet' diagram. It provides an additional third-order contribution to the β function.

The one-loop structure of the theory provides a renormalization to the interaction vertex, that is, to the coupling constant, by means of the two diagrams drawn in figure 7. The sums over Matsubara frequencies can be calculated by using the standard techniques described, for example, in [55]. In the low energy limit for the electrons from the leads (that is, if only excitations about the Fermi level are taken into account), the sum of the two diagrams is given by

$$\mathcal{D}_1 + \mathcal{D}_2 \approx -\mathrm{i}\frac{J^2}{8}\delta_{\gamma\gamma'}\{[\delta_{\sigma\sigma'}\delta_{\alpha\alpha'} + \tau^a_{\sigma\sigma'}\tau^a_{\alpha\alpha'}] + [-\delta_{\sigma\sigma'}\delta_{\alpha\alpha'} + \tau^a_{\sigma\sigma'}\tau^a_{\alpha\alpha'}]\}2\nu(0)\ln\left(\frac{D}{k_\mathrm{B}T}\right) \tag{58}$$

(D is an ultraviolet cut-off, identified with the width of the conduction band). The corresponding renormalization to the coupling constant J is easily worked out and is given by

$$\Delta^{(2)}J(T, D) = 2\nu(0)J^2\ln\left(\frac{D}{k_\mathrm{B}T}\right). \tag{59}$$

A careful analysis of the vertex renormalization at third order in J reveals that several third-order diagrams are already taken into account by the scaling equation generated by the second-order vertex correction, as discussed in [56]. The only 'new' contribution comes from the 'non-parquet' diagram shown in figure 8. Because of the loop over the fermions from the contacts, such a contribution carries an overall factor of K; that is, the diagram is proportional to the number of channels and the correction to the coupling constant up to third order in J is

$$\Delta^{(3)}J = (2\nu(0)J^2 - 2K(\nu(0))^2J^3)\ln\left(\frac{D}{k_\mathrm{B}T}\right). \tag{60}$$

Integration of the renormalization group equation for J provides

$$-\frac{1}{2j} + \frac{1}{2j_0} + \frac{K}{2}\ln\left[\frac{j}{j_0}\left(\frac{1-Kj_0}{1-Kj}\right)\right] = x - x_0, \tag{61}$$

where $j = \nu(0)J$ and $x = \ln(\frac{D}{k_\mathrm{B}T})$.

It is seen from equation (61) that the fixed point is reached at an intermediate coupling j^*. However, the perturbative RG analysis is not conclusive here, because even in the ordinary, single-channel, Kondo model an artificial intermediate coupling fixed point is produced when the perturbative RG equations are expanded to third order [56].

It is straightforward to infer the Kondo temperature T_K from equation (61). Usually T_K is defined as the temperature scale at which j becomes $\mathcal{O}(1)$. Following such a criterion, at $T = T_K$ we can neglect $1/j$ compared to $1/j_0$ and obtain the following approximate formula for T_K:

$$k_B T_K \approx D(j_0)^{\frac{K}{2}} e^{-\frac{1}{2j_0}}. \tag{62}$$

Equation (62) is quite general, in that it provides the value for the crossover temperature for any number of channels K. This proves that the way the system approaches the scale at which the perturbative analysis breaks down does not depend on the number of channels, except for a redefinition of the Kondo temperature. Hence, logarithmic divergencies are expected when approaching to the T_K, no matter what the number of channels is. In the next subsection we will analyse the $T = 0$ behaviour of such a system, and will see that it is dramatically different from the one-channel case as regards the fixed point properties.

7.2. Analysis at $T \sim 0$

Several techniques have been applied in order to get information about physical quantities around the fixed point in the Kondo regime in such a limit. Finite T corrections have been derived by means of bosonization techniques [57, 58], Bethe ansatz-like exact solutions [7] and conformal field theory (CFT) techniques [8]. Now, the CFT approach is extremely effective in calculating finite T corrections, Wilson ratios and other exact results concerning Green functions [8], but its starting point that charge, spin and 'flavour' quantum numbers are enough to identify a primary fermionic field in the theory leads to an inconsistency: the corresponding on-shell S matrix comes out to be 0. The solution to such a 'unitarity paradox' has been suggested by Ludwig and Maldacena [59], who introduced a fourth 'spin flavour' quantum number. So, while at the unitarity limit charge, spin and flavour do not change upon scattering off the impurity, the spin flavour changes, giving rise to one more scattering channel. Such an extra quantum number allows for an off-diagonal on-shell S matrix; therefore the unitarity paradox simply means that the diagonal elements of the S matrix with respect to the spin flavour number are 0. However, a theory of the unitarity limit, needed in order to compute, for instance, within a unified framework transport properties with finite T corrections, is not yet fully developed. In this subsection we briefly sketch the first steps taken in order to derive an appropriate scattering potential in the style of Noziéres, in the case of the two-channel spin $1/2$ overscreened Kondo effect. We follow an approach equivalent to the one used by Tsvelick [60]; that is, the introduction of a regularization procedure able to move the fixed point toward infinite coupling. Then, we go through a bosonization–refermionization procedure in order to account for the scattering processes with changing of the spin flavour. The bosonization procedure allows us to split the degrees of freedom involved in our problem: in this way we will show that the Kondo interaction involves only the spin and spin flavour degrees of freedom while the charge and flavour ones are fully decoupled. This remark is a crucial one because it makes it possible to derive a S matrix in the unitarity limit which turns out to be diagonal in any quantum number but the spin flavour; such an S matrix describes the whole system of dot and contacts.

In the following we discuss the case $K = 2, S = 1/2$, so we have two flavours of conduction electrons from an effectively one-dimensional conductor which interact with a localized spin $1/2$ magnetic impurity.

Let $c_{\alpha\sigma}(x)$ be the lead electron operators ($\sigma = \uparrow, \downarrow$ is the spin index, $\alpha = 1, 2$ is the flavour index). A lattice model complete Hamiltonian is written as

$$\begin{aligned} H^{2cH} = &-t \sum_x [c^\dagger_{\alpha\sigma}(x) c_{\alpha\sigma}(x+a) + c^\dagger_{\alpha\sigma}(x+a) c_{\alpha\sigma}(x)] \\ &- \mu \sum_x c^\dagger_{\alpha\sigma}(x) c_{\alpha\sigma}(x) + J \vec{S}_d \cdot [\vec{\sigma}_1(0) + \vec{\sigma}_2(0)] \end{aligned} \tag{63}$$

where $\vec{\sigma}_\alpha(x) = \frac{1}{2} c^\dagger_{\alpha\sigma}(x) \vec{\tau}_{\sigma\sigma'} c_{\alpha\sigma'}(x)$ and a is the lattice spacing.

Now, we can linearize the dispersion relation around the Fermi surface and introduce two chiral fields $c_{\pm,\alpha\sigma}(x)$. Even and odd parities can be introduced to obtain fields with the same chirality, $\phi^{\mathrm{e}}_{\alpha\sigma}$ and $\phi^{\mathrm{o}}_{\alpha\sigma}$, so odd parity fully decouples from the interaction Hamiltonian. In order to properly deal with the interacting fields, we will bosonize $\phi^{\mathrm{e}}_{\alpha\sigma}$; in particular, we define four bosonic fields $\Psi_{\alpha\sigma}$ in terms of which it is possible to express densities of the remarkable physical quantities. To this end we are led to construct the four bosonic fields Ψ_X ($X = \mathrm{ch}, \mathrm{sp}, \mathrm{fl}, \mathrm{sf}$) for the charge, spin, flavour and spin flavour degrees of freedom [58, 59, 61] as linear combinations of the previous ones.

In this way it is possible to realize two 'inequivalent' representations of the fields $\phi^{\mathrm{e}}_{\alpha\sigma}$ in terms of the fields Ψ_X ($X = \mathrm{ch}, \mathrm{sp}, \mathrm{fl}, \mathrm{sf}$), $\phi^{\mathrm{e}}_{\alpha\sigma;\mathrm{I}}$ and $\phi^{\mathrm{e}}_{\alpha\sigma;\mathrm{II}}$, given by

$$\begin{aligned}\phi^{\mathrm{e}}_{\alpha\sigma;\mathrm{I}}(x) &= \eta_{\alpha\sigma}{:}\mathrm{e}^{-\frac{\mathrm{i}}{2}[\Psi_{\mathrm{ch}}+\sigma\Psi_{\mathrm{sp}}+\alpha\Psi_{\mathrm{fl}}+\alpha\sigma\Psi_{\mathrm{sf}}](x)}{:},\\ \phi^{\mathrm{e}}_{\alpha\sigma;\mathrm{II}}(x) &= \xi_{\alpha\sigma}{:}\mathrm{e}^{-\frac{\mathrm{i}}{2}[\Psi_{\mathrm{ch}}+\sigma\Psi_{\mathrm{sp}}+\alpha\Psi_{\mathrm{fl}}-\alpha\sigma\Psi_{\mathrm{sf}}](x)}{:},\end{aligned} \tag{64}$$

where η and ξ are suitable Klein factors. Notice that the two fields differ only in the spin flavour quantum number but such a difference is a crucial one.

Now we are ready to rewrite the two-channel Kondo interaction Hamiltonian in bosonic coordinates Ψ_X as

$$\begin{aligned}H^{\mathrm{2cH}}_{\mathrm{K}} &= J\left\{S^{+}_{d}{:}\mathrm{e}^{-\mathrm{i}\Psi_{\mathrm{sp}}(0)}{::}\cos(\Psi_{\mathrm{sf}}(0)){:} + S^{-}_{d}{:}\mathrm{e}^{\mathrm{i}\Psi_{\mathrm{sp}}(0)}{::}\cos(\Psi_{\mathrm{sf}}(0)){:} + S^{z}_{d}\frac{L}{2\pi}\frac{\mathrm{d}\Psi_{\mathrm{sp}}(0)}{\mathrm{d}x}\right\}\\ &= J\vec{S}_d\cdot[\vec{\Sigma}_g(0)+\vec{\Sigma}_u(0)],\end{aligned} \tag{65}$$

where the spin densities $\vec{\Sigma}_{A,B}(x)$ are given by

$$\begin{aligned}\Sigma^{\pm}_{g}(x) &= {:}\mathrm{e}^{\pm\mathrm{i}[\Psi_{\mathrm{sp}}+\Psi_{\mathrm{sf}}](x)}{:}, \qquad & \Sigma^{z}_{g}(x) &= \frac{L}{4\pi}\frac{\mathrm{d}}{\mathrm{d}x}[\Psi_{\mathrm{sp}}+\Psi_{\mathrm{sf}}](x),\\ \Sigma^{\pm}_{u}(x) &= {:}\mathrm{e}^{\pm\mathrm{i}[\Psi_{\mathrm{sp}}-\Psi_{\mathrm{sf}}](x)}{:}, \qquad & \Sigma^{z}_{u}(x) &= \frac{L}{4\pi}\frac{\mathrm{d}}{\mathrm{d}x}[\Psi_{\mathrm{sp}}-\Psi_{\mathrm{sf}}](x).\end{aligned} \tag{66}$$

Both $\vec{\Sigma}_g(x)$ and $\vec{\Sigma}_u(x)$ are $SU(2)$ spin current operators, so the vector space is made up of the bosonic vacuum $|\mathrm{bvac}\rangle$ and the bosonic spin $1/2$ spinors at a point x:

$$\begin{aligned}|\sigma_g\rangle &\equiv {:}\mathrm{e}^{\sigma\frac{\mathrm{i}}{2}[\Psi_{\mathrm{sp}}+\Psi_{\mathrm{sf}}](x)}{:}|\mathrm{bvac}\rangle,\\ |\sigma_u\rangle &\equiv {:}\mathrm{e}^{\sigma\frac{\mathrm{i}}{2}[\Psi_{\mathrm{sp}}-\Psi_{\mathrm{sf}}](x)}{:}|\mathrm{bvac}\rangle.\end{aligned} \tag{67}$$

No triplet adding g and u spin species together can occur because, given $\vec{\Sigma}_{g,u} = \int_{-L/2}^{L/2}\mathrm{d}x\,\vec{\Sigma}_{g,u}(x)$, we have

$$\vec{\Sigma}_g|\sigma_u\rangle = 0 \qquad \vec{\Sigma}_u|\sigma_g\rangle = 0; \tag{68}$$

that is, if at a point x the spin density associated with $\vec{\Sigma}_g$ is $\neq 0$, then, at the same point, the spin density associated with $\vec{\Sigma}_u$ is $= 0$, and vice versa; this does not allow for overscreening. Such a statement is a crucial one; indeed it corresponds to a particular regularization scheme [60] able to move the finite coupling fixed point corresponding to the unitarity limit down to $J = +\infty$. At this infinitely strongly coupled fixed point the impurity spin will be fully screened in a localized spin singlet. In principle, the system might lie within any linear combination mixing the two representations g, u, of the form

$$|\mathrm{GS}\rangle_{\mu}|_{x=0} = |\Uparrow\rangle\otimes\tfrac{1}{2}(|\downarrow_{\mathrm{g}}\rangle+\mu|\downarrow_u\rangle)|_{x=0} - |\Downarrow\rangle\otimes\tfrac{1}{2}(|\uparrow_{\mathrm{g}}\rangle+\mu|\uparrow_u\rangle)|_{x=0}, \tag{69}$$

where $|\Uparrow\rangle$, $|\Downarrow\rangle$ are the two impurity states with opposite spin polarizations. Then we search for the two independent linear combinations that do not change upon scattering of lead electrons; it can be shown that such combinations correspond to the values $\mu = \pm\mathrm{i}$.

Now, in the fixed point limit, we 'refermionize'. Physical states mix both representations, I and II. Scattering by the impurity states should conserve all physical quantum numbers. It can be shown that the elastic scattering in the unitarity limit swaps the two inequivalent representations I–II of the lead electrons. Correspondingly, the impurity absorbs/emits one spin flavour quantum. The even parity S matrix has the following representation in the I–II space:

$$\mathbf{S}^0(\omega = 0) = \begin{pmatrix} 0 & -\mathrm{i} \\ \mathrm{i} & 0 \end{pmatrix} \equiv \begin{pmatrix} 0 & \mathrm{e}^{-\mathrm{i}\frac{\pi}{2}} \\ \mathrm{e}^{\mathrm{i}\frac{\pi}{2}} & 0 \end{pmatrix}. \tag{70}$$

According to equation (70) the phase shifts induced by the scattering are $\delta^{\mathrm{I\ II}}(\omega = 0) = -\frac{\pi}{4}$, $\delta^{\mathrm{II\ I}}(\omega = 0) = \frac{\pi}{4}$, while in the case of the one-channel spin $1/2$ Kondo effect the phase shift was $\delta^0 = \frac{\pi}{2}$. Finally, the conductance can be easily obtained from the Landauer formula using equation (70) and $\mathbf{S}^1 = -\mathbf{1}$:

$$g = \mathrm{Tr}\{\mathbf{T}\} = \mathrm{Tr}\left\{\left|\tfrac{1}{2}\sum_l S^l\right|^2\right\} = \tfrac{1}{2}\,\mathrm{Tr}\begin{pmatrix} 1 & \mathrm{i} \\ -\mathrm{i} & 1 \end{pmatrix} = 1. \tag{71}$$

Incidentally, we point out that the ground state degeneracy always decreases under renormalization, which is the content of the 'g-theorem' [8]. This leads to a zero-temperature entropy for the impurity given by $S_{\mathrm{imp}}(0) = \frac{1}{2}\ln 2$.

Temperature corrections to this result have also been calculated [60] by using real fermion coordinates (Majorana fermions) $\psi^a(x)$ $(a = 1, 2, 3)$, which obey the anticommutation relations $\{\psi^a(x), \psi^b(y)\} = \delta^{ab}\delta(x - y)$, describing the relevant coordinates only. This corresponds also to a regularization scheme where the fixed point has been moved to $J = \infty$. The $\sqrt{T}$ behaviour is recovered, as mentioned in the introduction to this section (see equation (52)).

7.3. Can we reach the two-channel Kondo fixed point in a quantum dot?

A possible experimental realization of the two-channel Kondo fixed point in a quantum dot has been recently proposed [24]: exact diagonalization results for a vertical quantum dot with five electrons show that it can be tuned, by means of a strong external magnetic field, at the degeneracy point between energy levels with $S = 1/2$, but with different orbital angular momentum. Vertical cylindrical contacts provide single-particle energy subbands labelled by the cross-sectional angular momentum and the k vector of the incoming/outgoing electron. Appropriate tuning of the electron density in the contacts offers the chance of including two electron channels only. The advantage of this setting is that no exchange coupling can take place between the channels due to symmetry, so they act as totally independent. Selection rules due to the cylindrical symmetry enforce angular momentum m conservation and spin component σ conservation in the cotunnelling processes. For the special setting of the proposed device only a hole (h) process for $\downarrow$ spin and a particle process for $\uparrow$ spin are allowed. They differ in the sign of the potential scattering but this difference is inessential. In fact, a particle–hole transformation on the fermion fields of the $\uparrow$ channel only reverses the unwanted sign without affecting the exchange coupling. This puts the two channels on an equal footing and points to an 'orbital' Kondo coupling where the spin acts as the label for the channel. At this stage the dot plays the role of an effective spin $3/2$ impurity, interacting with two channels. So, as it stands, the system would flow to an underscreened situation in lowering the temperature. However, provided that the Zeeman spin splitting Δ is larger than the Kondo temperature for the underscreened fixed point $T_{\mathrm{K}}^{\mathrm{u}}$, there is a crossover temperature T^{c} at which two of the four $S = 1/2$ states are ruled out of the cotunnelling processes, thus allowing for an effective spin $1/2$ two-channel Kondo flow.

Detecting the effect requires an appropriate control of the hybridization of the dot with the contacts (so $\Delta \gg T_K^u$) and a proper tuning of the gate voltage V_g. This allows for fine tuning of the exchange couplings between the dot and the two channels. It is well known that the hardest condition to realize is total equivalence of the channels in the coupling. Were this not the case, the system would prefer one of the two channels as the dominant one and flow to a more conventional one-channel Kondo state. By tuning V_g one can cross the point where the two channels are equally coupled which allows for scaling towards the two-channel fixed point. The measured conductance $g(T)$ versus T will exhibit quadratic behaviour at low temperature except for a crossover to a square root behaviour, at the appropriate V_g value which makes the two channels perfectly equivalent (see figure 6). The delicate point in this proposal is that the requirement of full cylindrical symmetry of the device is essential.

Another set-up for measuring the two-channel Kondo conductance has been proposed recently [25]. This proposal relies on an extra contact to provide the second channel. It is recognized however that this would introduce cross-exchange terms between the three leads which do not allow for equivalent coupling of the two channels. In fact, any diagonalization of the scattering problem of the kind of the one outlined in the previous subsection to isolate the independent channels can never produce equal coupling as long as off-diagonal terms are non-zero. To overcome this difficulty the authors propose that the extra contact is a larger dot itself, having a charging energy E_c which hinders exchange coupling with the other two leads. Of course its size should be appropriately tuned. A smaller size implies a larger level spacing δ inside it and δ should be low enough because it acts as the low energy cut-off in the scaling toward the fixed point. Therefore, there is a delicate trade-off between increasing E_c to prevent cross-exchange terms and decreasing δ so as not to stop the flow when reducing the temperature.

We have stressed that the NFL fixed point in the two-channel Kondo coupling at $T = 0$ can only be reached by tuning the exchange couplings of both channels J_1, J_2 exactly equally. One would hope that this can be done by changing an appropriate gate voltage across a critical point V_g^*. According to figure 4 the system flows to $J_1 \to \infty$, $J_2 \to 0$ for $V_g < V_{g^*}$ and to $J_2 \to \infty$, $J_1 \to 0$ for $V_g > V_{g^*}$, both of which are Fermi liquid fixed points. It has been argued that the quantum transition across V_g^* should display a quantum critical region in the $T-V_g$ plane whose critical properties can be determined [26]. This offers better chances to spot whether we are in the vicinity of the NFL fixed point or not, at finite temperature also.

8. Summary

In this review we focused on equilibrium transport properties across a quantum dot (QD). A QD is a tunnelling centre for electrons coming from the leads. Depending on the transparency of the barriers and on the temperature, the coupling V to the leads is weak or strong.

In the weak coupling regime, tunnelling can be dealt with perturbatively. In the case of the QD, a Coulomb blockade zone is delimited by two sharp conduction peaks which grow as $|V|^2/T$ on lowering the temperature. Conduction in between is due to cotunnelling processes and is exponentially damped in temperature. The differential conductance is quite small, being $\propto |V|^4/U$, so the charge degree of freedom is frozen on the dot.

On lowering the temperature, non-perturbative coupling of the dot to the delocalized electrons of the contacts can occur and conductance can reach the unitary limit in a CB valley. For pedagogical reasons we have reviewed the old-fashioned Anderson–Yuval model for the correlated state. Otherwise we have used the *poor man's scaling* approach in the regime where perturbative scaling applies and the Noziéres scattering approach which entails fixed point physics at zero temperature. These approaches do not allow for quantitative results which are better obtained with the numerical renormalization group (NRG), real time RG

and non-crossing approximation (NCA) (the latter preferably in the overscreened case when a non-Fermi liquid (NFL) fixed point is reached), but they offer a more transparent view of what is going on.

We have briefly reviewed the various types of Kondo coupling.

We have considered the case in which the GS of the dot is degenerate because of spin: if temperature is low enough ($T < T_K$, with T_K depending on the transparency of the barriers), spin flip processes proliferate and the magnetic moment of the dot is partially or fully screened. In this case an applied magnetic field has a disruptive effect on the Kondo peak of the conductance. The interesting case of a crossing between different dot spin states induced by the magnetic field has also been discussed.

We have also reported on other possible realizations of Kondo physics involving orbital degrees of freedom (orbital Kondo). The most favourable set-up for this case is a vertical geometry of the dot and the contacts with cylindrical symmetry. In this geometry a magnetic field orthogonal to the dot (which may be strong) can induce level crossings and produce the degeneracies of the dot GS which are required for Kondo conductance to take place. Hence one can also have a Kondo effect with an even number of electrons on the dot and zero total spin.

Some attention has been devoted to the multichannel Kondo effect. The overscreening case can lead to a NFL fixed point at zero temperature. In particular we have discussed the two-channel spin 1/2 Kondo state and reported on possible experimental realizations that have been proposed. It emerges that the conditions to be met are very tough. Nonetheless, the achievement would probe a beautiful piece of the physics of the strongly correlated systems.

Acknowledgments

This work is a revised and updated version of lectures delivered by one of us (AT) at INFN Laboratories in Frascati (Italy) during the school 'Nanotubes & Nanostructures' (18–27 October 2001). AT wishes to thank S Bellucci and M De Crescenzi for the invitation to work in such a warm and stimulating atmosphere. A Naddeo was supported by a CNR fellowship while this work was done.

Appendix A. RG equations for the Coulomb gas model of equation (29)

We summarize here the scaling of the action in equation (29) in order to find the behaviour of the system at large timescales (low temperature) [21, 34]. The cut-off is rescaled according to: $\tau_M \to (1+\lambda)\tau_M$ with $\lambda = \Delta\tau_M/\tau_M \to d\ln\tau_M$. This adds a factor $e^{-2N\lambda(1-\alpha^2/2)}$. The first term arises from τ_M^{2N} in the denominator, while the one $\propto\alpha^2$ arises from the ln term in the interaction term. Indeed charge neutrality implies that $0 = (\sum_i q_i)^2 = \sum_{i\neq j} q_i q_j + \sum_i q_i^2$ and $q_{i,j} = \pm 1$. This factor renormalizes the fugacity $Y \to Y + dY$, with

$$Y + dY \approx Y e^{\lambda(1-\alpha^2/2)}, \tag{72}$$

which gives the first of equation (30). The interaction strength α is renormalized by flip–antiflip (particle–antiparticle) fusion.

Let us consider now all the configurations in which pairs of neighbouring charges q_i at τ_i and $q_j = -q_i$ at τ_j (where $j = i \pm 1$) are at a distance between τ_M and $\tau_M(1+\lambda)$. On increasing the scale, these pairs are seen as a neutral compound which screens the interaction between other charges ('fusion' of pairs). Let us consider one single fusion process and develop that part of the action that contains their coordinates:

$$-S^{(2N+2)} = -S^{(2N)} + q_i q_j \ln\left|\frac{\epsilon}{\tau_M}\right| + \frac{q_i}{2}\sum_{k\neq i,j} q_k\left[\ln\left|\frac{\tau_k - \tau - \epsilon/2}{\tau_M}\right| - \ln\left|\frac{\tau_k - \tau + \epsilon/2}{\tau_M}\right|\right]. \tag{73}$$

Here we have defined $\epsilon/2 = \frac{\tau_i - \tau_j}{2}$ and $\tau = \frac{\tau_i + \tau_j}{2}$. The integral over τ and ϵ for $\epsilon/\tau_{\rm M} \ll 1$ which appears in the partition function of equation (29) is:

$$\mathrm{e}^{-S^{(2N)}} Y^2 \int_{\tau_{i-1}+\tau_{\rm M}}^{\tau_{j+1}-\tau_{\rm M}} \frac{\mathrm{d}\tau}{\tau_{\rm M}} \int_{\tau_{\rm M}}^{\tau_{\rm M}(1+\lambda)} \frac{\mathrm{d}\epsilon}{\tau_{\rm M}} \left(\frac{\epsilon}{\tau_{\rm M}}\right)^{-\alpha^2} \mathrm{e}^{-\alpha^2 \epsilon \frac{q_i}{2} \sum_{k\neq i,j} q_k \frac{\partial}{\partial \tau} \ln\left|\frac{(\tau_k - \tau)}{\tau_{\rm M}}\right|}$$

$$\sim \lambda Y^2 \left\{ 1 - \alpha^2 \left(\frac{q_{i-1}}{2} \sum_{k\neq i,j}^{2N} q_k \ln\left| \frac{\tau_{i-1} + (\tau_{\rm M} - \tau_k)}{\tau_{\rm M}} \right| \right.\right.$$

$$\left.\left. + \frac{q_{j+1}}{2} \sum_{k\neq i,j}^{2N} q_k \ln\left| \frac{\tau_{j+1} - (\tau_{\rm M} - \tau_k)}{\tau_{\rm M}} \right| \right) \right\}, \tag{74}$$

where the term with $k = i - 1$ ($k = j + 1$) in the first (second) sum vanishes. Doing the same for each interval $i - j$ and summing, each term is repeated twice. This generates an extra contribution to the action that can be interpreted as the renormalization of the coupling constant:

$$\alpha^2 \to \alpha^2 + \mathrm{d}\alpha^2; \qquad \mathrm{d}\alpha^2 = -2\lambda Y^2 \alpha^2. \tag{75}$$

Because $\lambda \approx \mathrm{d} \ln \tau_{\rm M}$, the second of equations (30) is obtained.

Appendix B. Temperature dependence of the conductance

Ohm's law can be derived semiclassically from a Boltzmann equation which accounts for weak scattering of the charge carriers against impurities and defects, when driven by an electric field. Scattering provides a mechanism for relaxation from a non-equilibrium to a steady state flow [62]. We follow here a simplified approach starting from the velocity of band electrons $\vec{v}_k = \vec{\nabla}\epsilon_k/\hbar$. The current density is

$$\vec{j} = -\frac{2e}{3\mathcal{V}} \sum_k \vec{v}_k (f_k - f_k^o) \tag{76}$$

where $f_k (f_k^o)$ is the non-equilibrium (equilibrium) Fermi distribution and $\mathcal{V}$ is the volume. Now we take

$$f_k - f_k^o = -\frac{\partial f^o}{\partial \epsilon_k} \delta\epsilon_k, \qquad \delta\epsilon_k = -e\vec{E} \cdot \vec{v}_k \tau(k), \tag{77}$$

which defines the relaxation time $\tau(k)$, so, according to Ohm's law, we get

$$\sigma = -\frac{2e^2}{3\mathcal{V}} \sum_k \vec{v}_k \cdot \vec{v}_k \tau(k) \frac{\partial f^o}{\partial \epsilon_k}. \tag{78}$$

In the case of s-wave scattering a spherical wave is diffracted from the impurity with maximum amplitude; this increases the flux propagating backward. Assuming that quantities depend on ϵ only and are mostly evaluated at the Fermi level we have ($T \sim 0$)

$$\sigma = -\frac{2e^2}{3\mathcal{V}} \nu(0) v_{\rm F}^2 \int \mathrm{d}\epsilon\, \tau(\epsilon, T) \frac{\partial f^o}{\partial \epsilon}. \tag{79}$$

In this way we recover the simple microscopic formula for Ohm's conductivity, first derived by Drude in 1900, $\sigma = ne^2\tau/m$, where τ is an average relaxation time. The latter can be defined in terms of the mean free path between two scattering events $l = v_{\rm F}\tau$ or distance between impurities. This formula is valid in the limit $k_{\rm F} l \gg 1$ which we assume to be the case. In such a limit no localization effects occur and one can show that $\mathrm{d}\rho/\mathrm{d}T > 0$ always, which is violated in the case of Kondo conductivity in dilute alloys.

In fact, for the large U Anderson model, the explicit dependence of the transport time on temperature at the Fermi energy has to be taken into account separately. In addition, the Sommerfeld expansion can be used at finite temperatures [10]:

$$\int \mathrm{d}\epsilon \left(-\frac{\partial f(\epsilon)}{\partial \epsilon}\right)\tau(\epsilon, T) = \tau(\mu, T) + \frac{\pi^2}{6}(k_\mathrm{B}T)^2 \frac{\mathrm{d}^2\tau}{\mathrm{d}\epsilon^2}\bigg|_{\epsilon=\mu}$$
$$= \tau(\mu, 0)\left[1 + \frac{\pi^2}{16T_\mathrm{K}^2}\left(\frac{1}{2}\pi^2T^2 + \frac{\pi^2}{6}3T^2\right)\right]. \tag{80}$$

The main ingredients used for deriving this formula are the Fermi liquid nature of the zero-temperature GS and the Taylor expansion of the temperature dependence of the relaxation time. The prefactors have been specialized to the case of the symmetric Anderson model (so that the lifetime of the Kondo resonance is $\Gamma = 4k_\mathrm{B}T_\mathrm{K}/\pi$).

It follows that, in dilute alloys, the resistivity takes a maximum at $T = 0$:

$$\frac{\rho(T)}{\rho(0)} = 1 - \frac{\pi^4T^2}{16T_\mathrm{K}^2}. \tag{81}$$

The extra correction on the rhs of equation (80) arises from inelastic scattering at finite temperature, as shown by Noziéres [40], according to the following argument.

In an elastic resonant scattering process at $T = 0$ is $-\mathrm{Im}\{t^0\} = \frac{1}{\nu(0)\pi}\sin^2\delta^0$. In a diffusive s-wave scattering at finite T, we have to consider the total relaxation rate, defined as

$$\frac{1}{\tau(\epsilon)} = \sum_{k'} w_{kk'}(1 - kk') = \frac{2\pi}{\hbar}N_\mathrm{i}\nu(0)\int \mathrm{d}\epsilon_{k'}\,\delta(\epsilon_k - \epsilon_{k'})|\langle k|t|k'\rangle|^2$$

(s-wave scattering implies that the correction kk' averages to zero). The inelasticity can be accounted for by defining an effective elastic S matrix which is now no longer unitary and an effective phase shift which is different from the one at $T = 0$.

The full S matrix, instead, is of course unitary: $1 = \sum_\beta |S_{\alpha\beta}|^2 \equiv \sum_\beta[\delta_{\alpha\beta} - 2\pi\mathrm{i}\nu(0)t_{\alpha\beta}\delta(\epsilon_\alpha - \epsilon_\beta)][\delta_{\alpha\beta} + 2\pi\mathrm{i}\nu(0)t^*_{\alpha\beta}\delta(\epsilon_\alpha - \epsilon_\beta)] = \sum_\beta \delta_{\alpha\beta} + \sum_\beta 4\pi^2(\nu(0))^2|t_{\alpha\beta}|^2\delta(\epsilon_\alpha - \epsilon_\beta)$. Now, we separate the elastic channels $\beta = \alpha$ from the inelastic ones on the rhs and we introduce the inelastic cross-section $W_\alpha^{\mathrm{in}} = 2\pi\sum_{\beta\neq\alpha}\nu(0)|t_{\alpha\beta}|^2\delta(\epsilon_\alpha - \epsilon_\beta)$; hence, from unitarity it follows that $1 + 4\pi^2(\nu(0))^2|t_{\alpha\alpha}|^2 + 2\pi\nu(0)W_\alpha^{\mathrm{in}} = 1$. Thus, we can define an effective phase shift (which we call δ again) in the presence of inelastic scattering by introducing an effective 'elastic' S matrix:

$$1 - 2\pi\mathrm{i}\nu(0)t_{\alpha\alpha} = (1 - 2\pi\nu(0)W_\alpha^{\mathrm{in}})^{\frac{1}{2}}\mathrm{e}^{2\mathrm{i}\delta}, \tag{82}$$

where the square root can be expanded.

According to the optical theorem, we can write the total transmission probability as

$$W_\alpha = -2\,\mathrm{Im}\{t_{\alpha\alpha}\} = W_\alpha^{\mathrm{in}}\cos 2\delta + \frac{(1 - \cos 2\delta)}{\nu(0)\pi}. \tag{83}$$

Now, let us note that, because $\delta \sim \pi/2$, we have $\cos 2\delta < 0$. Therefore, for each channel α the quantity W_α is always smaller than the elastic case value: $2\sin^2\delta/(\nu(0)\pi)$. But one can thermally average over the α channels; according to the usual phase space argument which is invoked when scattering occurs close to the Fermi surface at very low T, we obtain an average $\overline{W^{\mathrm{in}}}$ proportional to T^2: $\overline{W^{\mathrm{in}}} \sim AT^2$. This gives rise to the first term in the expansion of equation (80). The second term can be viewed as contributing to the Sommerfeld expansion with $\delta(\epsilon) = \frac{1}{2}\pi - a\epsilon$ from which it follows that $\sin^2\delta \sim 1 - a^2\epsilon^2$.

In the case of resonant tunnelling across the dot, the conductance is given by equation (20). Using the result of equation (83) directly, one obtains that the conductance has a maximum at zero temperature and the first corrections in temperature are again $\mathcal{O}(T^2)$ (see equation (49)).

References

[1] Glazman L I and Raikh M E 1988 *Pis. Zh. Eksp. Teor. Fiz.* **47** 378
Glazman L I and Raikh M E 1988 *JETP Lett.* **47** 452 (Engl. Transl.)
[2] Aleiner I L, Brouwer P W and Glazman L I 2002 *Phys. Rep.* **358** 309
[3] Goldhaber-Gordon D, Shtrikman H, Mahalu D, Abusch-Magder D, Meirav U and Kastner M A 1998 *Nature* **391** 156
Cronenwett S M, Oosterkamp T H and Kouwenhoven L P 1998 *Science* **281** 540
Schmid J, Weis J, Eberl K and Klitzing K v 1998 *Physica* B **256–258** 182
Sasaki S, De Franceschi S, Elzerman J M, van der Wiel W G, Eto M, Tarucha S and Kouwenhoven L P 2000 *Nature* **405** 764
[4] Kondo J 1964 *Prog. Theor. Phys.* **32** 37
[5] Hewson A C 1993 *The Kondo Effect to Heavy Fermions* (Cambridge: Cambridge University Press)
[6] Wilson K G 1975 *Rev. Mod. Phys.* **47** 773
Krishnamurthy H R, Wilkins J W and Wilson K G 1980 *Phys. Rev.* B **21** 1003
[7] Tsvelick A M and Wiegmann P B 1983 *Adv. Phys.* **32** 453
Konik R M, Saleur H and Ludwig A W W 2001 *Phys. Rev. Lett.* **87** 236801
Konik R M, Saleur H and Ludwig A W W 2002 *Phys. Rev.* B **66** 125304
[8] Affleck I and Ludwig A W W 1993 *Phys. Rev.* B **48** 7297
Affleck I and Ludwig A W W 1991 *Nucl. Phys.* B **352** 849
Affleck I and Ludwig A W W 1991 *Nucl. Phys.* B **360** 641
Affleck I and Ludwig A W W 1991 *Phys. Rev. Lett.* **67** 161
Affleck I 1995 *Acta Phys. Pol.* B **26** 1869
[9] Bickers N E 1987 *Rev. Mod. Phys.* **59** 845
[10] Costi T A, Hewson A C and Zlatic V 1994 *J. Phys.: Condens. Matter* **6** 2519
Costi T A and Hewson A C 1992 *Phil. Mag.* B **65** 1165
[11] Costi T A 2001 *Phys. Rev.* B **64** 24130(R)
Costi T A 2000 *Phys. Rev. Lett.* **85** 1504
[12] Sakai O and Shimizu Y 1992 *J. Phys. Soc. Japan* **61** 2333
Sakai O, Suzuki S and Shimizu Y 1995 *Physica* B **206–207** 141
Izumida W, Sakai O and Shimizu Y 1997 *J. Phys. Soc. Japan* **66** 717
Izumida W, Sakai O and Shimizu Y 1998 *J. Phys. Soc. Japan* **67** 2444
[13] Ng T K 1988 *Phys. Rev. Lett.* **61** 1768
[14] Hershfield S, Davies J H and Wilkins J W 1991 *Phys. Rev. Lett.* **67** 3270
Levy Yeyati A, Martin-Rodero A and Flores F 1993 *Phys. Rev. Lett.* **71** 2991
Oguri A 2001 *Phys. Rev.* B **64** 153305
Takagi O and Saso T 1999 *J. Phys. Soc. Japan* **68** 2894
[15] Meir Y, Wingreen N S and Lee P A 1993 *Phys. Rev. Lett.* **70** 2601
Meir Y and Wingreen N S 1992 *Phys. Rev. Lett.* **68** 2512
[16] Koenig J, Schmidt J, Schoeller H and Schon G 1996 *Phys. Rev.* B **54** 16820
Koenig J, Schmidt J, Schoeller H and Schon G 1996 *Czech. J. Phys.* **46** 2399
[17] Meir Y and Wingreen N S 1994 *Phys. Rev.* B **49** 11040
[18] Hettler M H, Kroha J and Hershfield S 1998 *Phys. Rev.* B **58** 5649
[19] Schoeller H and Schon G 1994 *Phys. Rev.* B **50** 18436
Schoeller H 1997 *Mesoscopic Electron Transport* (*NATO ASI Series E* vol 345) vol 105, ed L Sohn, L P Kouwenhoven and G Schön (Dordrecht: Kluwer) pp 291–330
Schoeller H 2000 *Lecture Notes in Physics* vol 544 (Heidelberg: Springer) p 137
[20] Schoeller H and Koenig J 2000 *Phys. Rev. Lett.* **84** 3686
Koenig J and Schoeller H 1998 *Phys. Rev. Lett.* **81** 3511
[21] Anderson P W, Yuval G and Hamann D R 1970 *Phys. Rev.* B **1** 4464
Hamann D R 1970 *Phys. Rev.* B **2** 1373
[22] Glazman L I and Pustilnik M 2002 *Proc. NATO ASI New Directions in Mesoscopic Physics (Erice, 2002)* at press
(Glazman L I and Pustilnik M 2003 *Preprint* cond-mat/0302159)
[23] Giuliano D, Jouault B and Tagliacozzo A 2001 *Phys. Rev.* B **63** 125318
Giuliano D, Jouault B and Tagliacozzo A 2001 *Macroscopic Quantum Coherence and Quantum Computing* ed D V Averin *et al* (New York: Kluwer–Academic) p 325
[24] Giuliano D, Jouault B and Tagliacozzo A 2002 *Europhys. Lett.* **58** 401
[25] Oreg Y and Goldhaber-Gordon D 2003 *Phys. Rev. Lett.* **90** 136602

[26] Glazman L I and Pustilnik M 2003 *Phys. Rev. Lett.* **91** 066405
[27] Kouwenhoven L P *et al* 1997 *Mesoscopic Electron Transport* (*NATO ASI Series E* vol 345) vol 105, ed L Sohn, L P Kouwenhoven and G Schön (Dordrecht: Kluwer)
[28] Jouault B, Santoro G and Tagliacozzo A 2000 *Phys. Rev.* B **61** 10242
[29] Kastner M A and Goldhaber-Gordon D 2001 *Solid State Commun.* **119** 245
[30] Ng T K and Lee P A 1988 *Phys. Rev. Lett.* **61** 1768
[31] Jauho A P, Wingreen N S and Meir Y 1994 *Phys. Rev.* B **50** 5528
[32] Keldysh L V 1965 *Zh. Eksp. Teor. Fiz.* **47** 1515
Keldysh L V 1965 *Sov. Phys.—JETP* **20** 1018 (Engl. Transl.)
Mahan G D 1990 *Many-Particle Physics* 2nd edn (New York: Plenum)
[33] Tagliacozzo A and Tosatti E 1988 *Phys. Scr.* **38** 301
[34] Nienhuis B 1987 *Coulomb Gas Formulation of Two-dimensional Phase Transitions* ed C Domb and J Lebowitz (New York: Academic)
[35] Giuliano D and Tagliacozzo A 2000 *Phys. Rev. Lett.* **84** 4677
[36] Kondo J 1966 *J. Appl. Phys.* **37** 1177
[37] van der Wiel W G, De Franceschi S, Fujisawa T, Elzerman J M, Tarucha S and Kouwenhoven L P 2000 *Science* **289** 2105
[38] Schrieffer J R and Wolff P A 1966 *Phys. Rev.* **149** 491
[39] Anderson P W 1970 *J. Phys. C: Solid State Phys.* C **3** 2436
[40] Noziéres P 1974 *J. Low Temp. Phys.* **17** 31
[41] Nozierés P and Blandin A 1980 *J. Physique* **41** 193
[42] Fabrizio M, Gogolin A O and Noziéres P 1995 *Phys. Rev.* B **51** 16088
[43] Andrei N 1982 *Phys. Lett.* A **87** 299
Andrei N, Furuya K and Lowenstein J H 1983 *Rev. Mod. Phys.* **55** 331
[44] Ovchinnikov Yu N and Dyugaev A M 1999 *JETP Lett.* **70** 111
Ovchinnikov Yu N and Dyugaev A M 1999 *JETP Lett.* **88** 696
[45] Tarucha S, Hausting D G, Honda T, van der Hage R J and Kouwenhoven L P 1996 *Phys. Rev. Lett.* **77** 3613
[46] Eto M and Nazarov Y 2000 *Phys. Rev. Lett.* **85** 1306
[47] Pustilnik M, Glazman L I, Cobden D H and Kouwenhoven L P 2001 *Lecture Notes in Physics* vol 579 (Heidelberg: Springer) p 3
Pustilnik M and Glazman L I 2001 *Phys. Rev. Lett.* **85** 2993
Pustilnik M and Glazman L I 2001 *Phys. Rev.* B **64** 045328
[48] Affleck I, Ludwig A W W and Jones B A 1995 *Phys. Rev.* B **52** 9528
[49] Wagner M, Merkt U and Chaplik A V 1992 *Phys. Rev.* B **45** 1951
Lucignano P, Jouault B and Tagliacozzo A 2004 *Phys. Rev.* B **69** 045314
[50] Ralph D C, Ludwig A W W, von Delft J and Buhrman R A 1994 *Phys. Rev. Lett.* **72** 1064
Upadhyay S K, Louie R N and Buhrman R A 1997 *Phys. Rev.* B **56** 12033
[51] Zaránd G and Zawadowsky A 1994 *Phys. Rev. Lett.* **72** 542
Zaránd G and Zawadowsky A 1994 *Phys. Rev.* B **50** 932
Cox D L and Zawadowsky A 1998 *Adv. Phys.* **47** 599
[52] Aleiner I L, Altshuler B L and Galperin Y M 2001 *Preprint* cond-mat 0102513
[53] Hettler M H, Kroha J and Hershfield S 1994 *Phys. Rev. Lett.* **73** 1967
[54] Luttinger J M 1960 *Phys. Rev.* **121** 942
[55] Fetter A L and Walecka J D 1981 *Quantum Theory of Many-Particle Systems* (New York: McGraw-Hill)
[56] Vladar K and Zawadowsky A 1983 *Phys. Rev.* B **28** 1564
Vladar K and Zawadowsky A 1983 *Phys. Rev.* B **28** 1582
Vladar K and Zawadowsky A 1983 *Phys. Rev.* B **28** 1596
[57] Muramatsu A and Guinea F 1986 *Phys. Rev. Lett.* **57** 2337
[58] Emery V J and Kivelson S 1992 *Phys. Rev.* B **46** 10812
Emery V J and Kivelson S 1993 *Phys. Rev. Lett.* **71** 3701
[59] Maldacena J M and Ludwig A W W 1997 *Nucl. Phys.* B **506** 565
[60] Coleman P, Ioffe L and Tsvelick A M 1995 *Phys. Rev.* B **52** 6611
[61] von Delft J, Zaránd G and Fabrizio M 1998 *Phys. Rev. Lett.* **81** 196
[62] Ashcroft N W and Mermin N D 1976 *Solid State Physics* (Tokyo: Holt-Saunders International Editions)